Tutor

Dr. Joaquín F. Pérez de Benito
Departament de Ciència de Materials i Química Física

Grau de Química

Treball Final de Grau

Complexation of chromium(III) by L-alanine: a kinetic study
Complexació de crom(III) per L-alanina: un estudi cinètic

Guillem Martínez Cereza

June 2018

Universitat de Barcelona

B:KC Barcelona Knowledge Campus
Campus d'Excel·lència Internacional

Nature is always more subtle, more intricate, more elegant than what we are able to imagine.

Carl Sagan

First of all, I would like to thank Dr. Joaquín F. Pérez de Benito for the dedication he has shown to me, as well as for the willingness to share with students his knowledge of chemistry, making easier the realization of this project.

I am also indebted to my parents and girlfriend for believing in me since I began this trip, and for their patience and the unconditional support generously offered when this work was still far from seeing the light. It would have not been the same without them.

REPORT

CONTENTS

1. SUMMARY

The kinetics of the reaction of substitution of aqua ligands in chromium(III) complexes by L-alanine has been studied with the aid of a spectrophotometric technique in aqueous media under slightly acidic conditions (pH 3.55 – 5.61). The process did not follow the usual pseudo-first order pattern, even under a large excess of amino acid with respect to the metal ion. On the contrary, the rate decreased much faster than a pseudo-first order reaction would. A two consecutive reaction model has been applied involving the formation (rate constant k_1) and decay (rate constant k_2) of a long-lived intermediate. Both rate constants decreased with the initial concentration of Cr(III) (due to the pH decrease) and increased with the initial concentration of organic ligand (fractional orders), whereas an increase of the medium ionic strength resulted in an increase of k_1 and a decrease of k_2, both steps presenting base catalysis and the corresponding activation energies being 60.2 ± 3.3 and 83.3 ± 5.9 kJ mol^{-1}. The rate constants for the replacement of an aqua ligand by L-alanine at 25.0 ºC followed the sequence $CrOH^{2+}$ (1.77 M^{-1} s^{-1}) < $Cr(OH)_2^+$ (128 M^{-1} s^{-1}) < $Cr(OH)_3$ (3.07×10^4 M^{-1} s^{-1}). The UV-Vis spectrum of the long-lived intermediate was intermediary between those of the inorganic reactant and the reaction product. The spectra of the final reacting mixtures revealed the co-existence of at least four different complexes in equilibrium. A mechanism in agreement with the available experimental data has been proposed, involving an elementary reaction sequence for each experimental rate constant, and starting both with the breakage of a Cr(III)-aqua chemical bond as a previous (slow) step to the coordination of the organic ligand.

Keywords: chromium(III), complexation reaction, kinetics, L-alanine, long-lived intermediate.

2. RESUM

La cinètica de la reacció de substitució dels lligands aqua per L-alanina en els complexes de crom(III) s'ha estudiat amb l'ajut d'una tècnica espectrofotomètrica en medi aquós sota condicions lleugerament acides (pH 3.55 – 5.61). El procés no va seguir el comportament de pseudo-primer ordre habitual, encara que fos amb un fort excés d'aminoàcid respecte l'ió metàl·lic. Pel contrari, la velocitat va disminuir molt més ràpid de com ho faria una reacció de pseudo-primer ordre. Un model de dues reaccions consecutives s'ha aplicat, implicant la formació (constant de velocitat k_1) i la destrucció (constant de velocitat k_2) d'un intermedi de llarga vida. Ambdues constants de velocitat van disminuir amb la concentració inicial de Cr(III) (degut a la baixada de pH) i van augmentar amb la concentració inicial del lligand orgànic (ordres fraccionaris), mentre que un augment de la força iònica del medi va resultar en un augment de k_1 i una disminució de k_2, presentant ambdues etapes catàlisis bàsica i sent les seves corresponents energies d'activació 60.2 ± 3.3 i 83.3 ± 5.9 kJ mol^{-1}. Les constants de velocitat d'intercanvi d'un lligand aqua per L-alanina a 25ºC van seguir la seqüència $CrOH^{2+}$ (1.77 M^{-1} s^{-1}) < $Cr(OH)_2^+$ (128 M^{-1} s^{-1}) < $Cr(OH)_3$ (3.07 × 10^4 M^{-1} s^{-1}). L'espectre UV-Vis del intermedi de llarga vida va ser intermedi entre els del reactiu inorgànic i el producte final. L'espectre de la mescla reactiva final a revelat la coexistència d'almenys quatre complexes diferents en equilibri. S'ha proposat un mecanisme de reacció coherent amb les dades experimentals disponibles, involucrant una seqüència de reaccions elementals per cada constant de velocitat experimental, i començant ambdues per la ruptura d'un enllaç químic Cr(III)-aqua com una etapa prèvia (lenta) a la coordinació amb el lligand orgànic.

Paraules clau: cinètica, crom(III), intermedi de llarga vida, L-alanina, reacció de complexació

3. INTRODUCTION

The coordination chemistry of chromium(III) differs from those of other transition metal ions in the rate of the reaction between the metal and its ligands. Whereas chemists are used to see in their laboratories how typical complexes such as tetraamminecopper(II) or diamminesilver(I) ions form in a rather fast way, and kinetic studies of the substitution of coordinated water on Pt(II) and many other metal ions by organic ligands often require the use of rapid reactant mixing techniques as the stopped-flow method,[1] the characteristic kinetic inertness to substitution of the Cr(III) d^2sp^3 octahedrical complexes[2,3] makes them especially attractive candidates to be employed in kinetic studies affordable by ordinary UV-Vis spectroscopy. For instance, the relatively slow reaction between Cr(III) and ethylenediaminetetraacetic acid (EDTA)[4,5] is selected as an adequate experiment in chemical kinetics for undergraduate students in some university faculties around the world.[6,7]

The complexes of Cr(III) are of certain importance in biology. Actually, chromium is nowadays considered by many authors as a necessary nutritional oligoelement[8] because of its participation in the glucose tolerance factor.[9-12] Although the classification as an essential trace element remains polemical,[13,14] the capacity of chromium to potentiate the action of insulin is well established.[15]

On the other hand, L-alanine, the simplest α-amino acid presenting optical isomerism, is classified as one of the 10 non-essential biological amino acids for humans, due to their ability to produce it.[16] Given that the amino acid molecules exhibit two functional groups with nitrogen and oxygen atoms capable of acting as electron-pair donors, they can be considered as suitable ligands for vacant-orbital transition metal ions. In particular, the reactions of complexation of Cr(III) by amino acids might be related to the problem of the origin of the first peptides on prebiotic Earth,[17] since transition metal ions have been shown to catalyze the formation of peptide bonds between the amino acid monomers acting as ligands.[18]

The substitution reactions on aqua,[19-26] hydroxo[27] and ammonia[28] complexes of Cr(III) by amino acids have been the subject of several kinetic studies. Although the results of two independent investigations of the Cr(III)-alanine reaction have already been reported,[29,30] the process under a large excess of organic ligand being classified in both cases as a pseudo-first order reaction, some clear-cut deviations from this simple kinetic behavior have been observed.

The main objective of the present work will be to search for and eventually find a kinetic model capable of accounting for those deviations.

4. OBJECTIVES

First: experiments. Given that the reaction rate is a function of many variables, in order to hold the complexity of the mathematical problem as low as possible, only one of them will be studied at each time. To that end, several series of kinetic runs will be designed and carried out, and in each of them a single experimental variable will be changed, keeping the remaining ones constant.

Second: calculations. One of the major problems when dealing with kinetic studies of ligand replacement on substitution inert metal centers as Cr(III) is the participation of long-lived intermediates in the mechanism. These intermediates are not reactive enough for the steady-state approximation to hold. Consequently, simple kinetic models involving a single rate constant (as the pseudo-first order model) are useless as far as these reactions are concerned. In the present study, a BASIC program will be developed to fit the experimental absorbance-time data with four fitting parameters: the initial absorbance, the molar absorption coefficient of a long-lived intermediate and two rate constants. In this way, it is hoped that enough information on the reaction at the macroscopic level will be accumulated to allow a solid elucidation of its microscopic aspects.

Third: mechanism. Once both the experiments and the calculations are done, a sequence of elementary reaction steps, being at the same time coherent with the available kinetic data and reasonable from a chemical perspective, will be looked for.

However, given the asymptotic character of the approach of science to the real behavior of nature, we should bear in mind that the best a scientist can hope for is to come near the truth as much as possible, but never reaching the truth itself.

5. EXPERIMENTAL SECTION

5.1. MATERIALS AND METHODS

All the experiments were done using as solvent water previously purified by deionization followed by treatment with a Millipore Synergy UV system (milli-Q quality, κ = 0.05 μS/cm at 25.0 ºC). The reactants required to carry out the kinetic runs were chromium(III) nitrate nonahydrate [$Cr(NO_3)_3 \cdot 9H_2O$, Merck, purity ≥ 98.0%] and alanine [CH_3-CH(NH_2)-COOH, Sigma-Aldrich] in its L [purity ≥ 99.5%] and DL [purity ≥ 99.0%] forms. Potassium hydroxide (KOH, Merck, purity ≥ 85%) was employed to perform the reaction at an adequate pH range. Actually, the window of accessible pHs was rather narrow, being limited at the bottom by the rate of reaction (too slow under very acidic conditions) and at the top by the eventual precipitation of $Cr(OH)_3$. The ionic strength was varied in some experiments by addition of potassium nitrate (KNO_3, Merck, purity ≥ 99.0%).

The pH measurements were done by means of a Wave pH-meter, provided with a digital presentation until the second decimal figure (± 0.01 pH) and a combination electrode, calibrated with the aid of commercial buffers of known pH (4.00 and 7.00, Sigma-Aldrich). The temperature was kept constant by means of a thermostatic bath provided with a digital reading (± 0.1 ºC). The kinetic runs were followed measuring periodically the absorbances either at five different wavelengths with a Shimadzu 160 A UV-Vis spectrophotometer (± 0.001 *A*) or at a single wavelength with a Shimadzu UV-1201V spectrophotometer (± 0.001 *A*). At the end of the reactions, the UV-Vis spectra (wavelength: 320-700 nm) corresponding to the final reaction products were recorded with the aid of a third spectrophotometer (SI Analytics, UV Line 8100 model).

5.2. KINETIC EXPERIMENTS AND CALCULATIONS

In most of the runs, the complexing agent, L-alanine, was in large excess with respect to the metal ion, the limiting reactant Cr(III), in order to attain an approximately constant (time independent) concentration of the organic ligand (isolation method). The total solution volume was kept the same in all the experiments (51 mL). In order to minimize the experimental errors associated with the kinetic data, the wavelength used to monitor the reaction was chosen as that leading to a higher increment of the solution absorbance between the initial and final points. Usually, the selected optimal wavelength was that of 530 nm. The absorbances of the reacting

mixture were periodically measured (time intervals: 60-360 s) during at least 6 hours, and the final values, along with the UV-Vis spectrum and the pH, were taken 4 days later (higher delay times were not advisable because of the potential contamination by fungal colonies feeding on the amino acid). With the objective to confirm the reproducibility of the kinetic determinations, all the experiments were duplicated. In total, 63 kinetic runs were performed.

The hardware used in the present work was a Sony Vaio personal computer, the software employed for the calculations was the programming language BBC BASIC (version for Windows) and for the graphics the program KaleidaGraph (version 4.03).

6. SPECTROPHOTOMETRIC MONITORING OF THE REACTION

The stock aqueous solution of $Cr(NO_3)_3$ (0.3 M, pH 2.01) exhibited a distinct blue color. Addition of an aliquot to an aqueous mixture of L-alanine and KOH resulted usually in precipitation of $Cr(OH)_3$, which redissolved rapidly on stirring, yielding a perfectly transparent green solution, whose color shifted gradually to violet as the complexation reaction advanced.

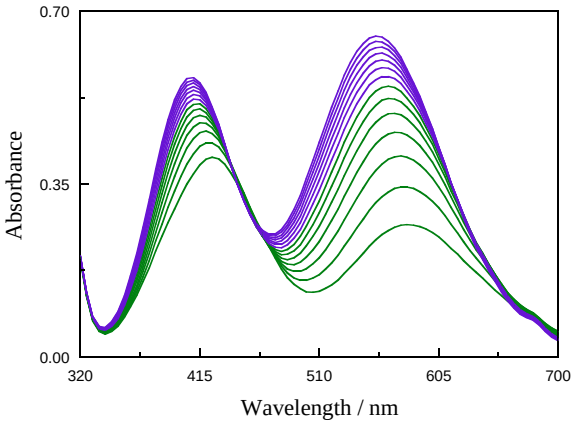

Figure 1. Periodic scanning of the UV-Vis spectrum at 30-min time intervals during the course of the process. The shift from green to violet indicates the progress of the reaction from reactants to products. $[Cr(NO_3)_3]_0 = 1.76 \times 10^{-2}$ M, [L-alanine]$_0$ = 0.354 M, $[KOH]_0 = 5.03 \times 10^{-3}$ M, pH_∞ 3.71, 25.0 ºC.

The absorbance of the solution increased at most wavelengths of the UV-Vis spectrum during the course of the reaction, and two absorption peaks shifting gradually toward the left side could be observed (Figure 1). The higher increase of the absorbance was that corresponding to the peak situated at the higher wavelength, thus being the best choice to follow the reaction keeping the experimental errors as low as possible.

In certain kinetic studies, when the reaction has been followed by a spectrophotometric technique determining simultaneously the absorbances at two different wavelengths, a representation of the absorbance at one wavelength, $A(\lambda_1)$, as a function of the other, $A(\lambda_2)$, can yield some useful information on the chemical system under study, for instance, on the participation of a long-lived intermediate (as opposed to very reactive, steady-state intermediates[31-33]) in the mechanism[5] or the colloidal nature of one of the reaction products.[34-36] In the particular case of the Cr(III)-alanine reaction, the absorbance (λ_1) - absorbance (λ_2) plots led to either downward-concave (λ_1 = 585 nm, λ_2 = 530 nm) or upward-concave (λ_1 = 400 nm, λ_2 = 530 nm) curves (Figure 2), thus suggesting the participation of at least a long-lived intermediate in the mechanism.

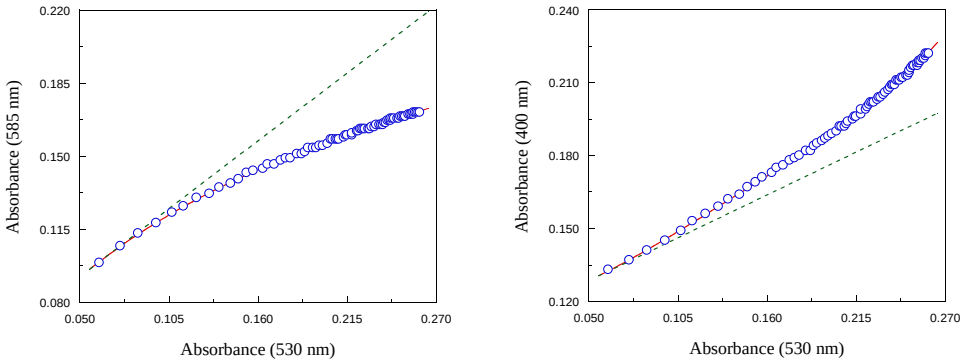

Figure 2. Absorbances at 585 (left) and 400 (right) nm as a function of the absorbance at 530 nm during the course of the reaction. The dashed lines are the tangents to the curves at the beginning of the reaction. $[Cr(NO_3)_3]_o$ = 5.88 × 10^{-3} M, $[\text{L-alanine}]_o$ = 0.133 M, $[KOH]_o$ = 8.28 × 10^{-3} M, pH_∞ 3.97, 25.0 ºC.

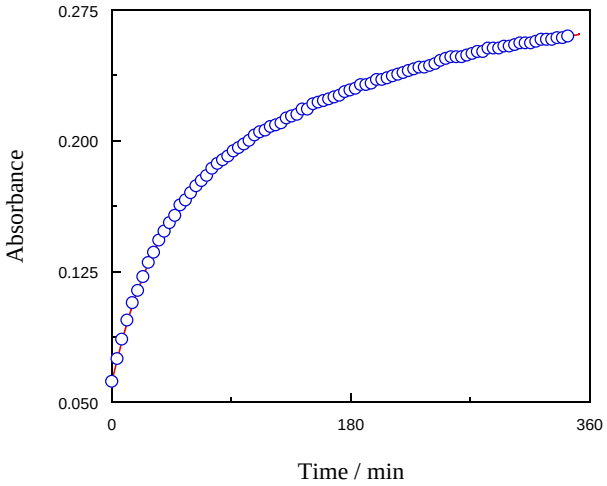

Figure 3. Absorbance at 530 nm as a function of time during the course of the reaction. $[Cr(NO_3)_3]_o$ = 5.88 $\times 10^{-3}$ M, $[\text{L-alanine}]_o$ = 0.133 M, $[KOH]_o$ = 8.28 $\times 10^{-3}$ M, pH_∞ 3.97, 25.0 ºC.

In all the cases, the absorbance-time plots presented a downward-concave curvature, meaning that the reaction rate decreased right from the beginning of the process. A typical example is shown in Figure 3. This behavior contrasts with that exhibited by one related reaction, the complexation of Cr(III) with EDTA, for which sigmoidal (S-shaped) absorbance vs. time and autocatalytic-like (bell-shaped) rate vs. time plots were found.[5]

7. ATTEMPTED PSEUDO-FIRST ORDER MODEL

The values of the reaction rate were obtained by means of the finite difference method. This mathematical procedure of approximate derivation in combination with the formula of the additive properties[32] allows the calculation of the rate at time $t + \Delta t/2$ from the absorbances at times t and $t + \Delta t$ as:

$$v_t \approx \frac{1}{A_\infty - A_o} \frac{A(t + \Delta t) - A(t)}{\Delta t} [R]_o \qquad (1)$$

A_o, $A(t)$, $A(t+\Delta t)$ and A_∞ being the absorbances at times 0, t, $t + \Delta t$ and ∞, respectively, whereas $[R]_o$ stands for the initial concentration of the limiting reactant. Equation 1 leads to reaction rate values with a very low systematic error provided that the time interval chosen (Δt) is small enough.

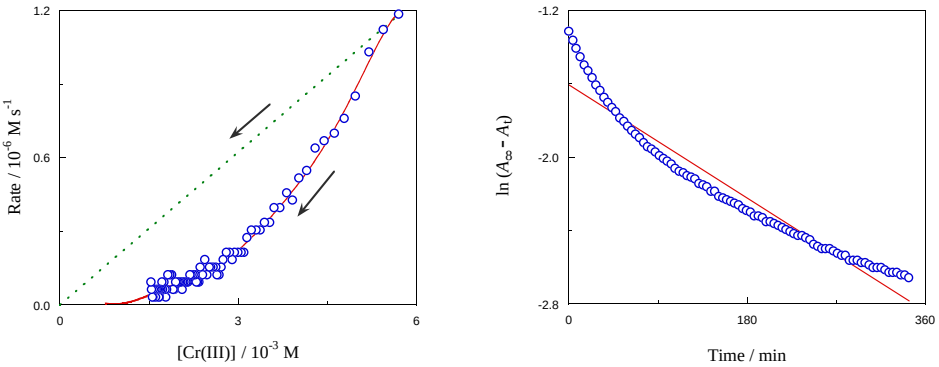

Figure 4. Left: Reaction rate as a function of the limiting reactant concentration. The dashed line corresponds to a hypothetical pseudo-first order behavior, whereas the arrows indicate the progression of the complexation process. Right: Attempted pseudo-first order plot. $[Cr(NO_3)_3]_o$ = 5.88 × 10^{-3} M, [L-alanine]$_o$ = 0.133 M, $[KOH]_o$ = 8.28 × 10^{-3} M, pH_∞ 3.97, 25.0 ºC.

The reaction rate so obtained has been plotted against the inorganic reactant concentration for a typical kinetic run in Figure 4 (left). It can be observed that the decrease of the rate did not follow a typical pseudo-first order pattern, as reported by other authors.[29,30] Actually, the rate-concentration curve was tangent to the straight line corresponding to the pseudo-first order behavior at the beginning of the process, but afterward the velocity started to decrease much faster than the limiting reactant concentration did. Moreover, the experimental absorbance-time data corresponding to the same experiment have been plotted on a pseudo-first order ln (A_∞-A_t) vs. t plane (Figure 4, right), yielding a clear-cut upward-concave curve instead of a straight line. Therefore, the simple pseudo-first order kinetic model has to be definitively rejected. We can conclude from the former plots that this situation calls for a kinetic model capable of explaining the slowing-down excess detected for the reaction.

8. CONSECUTIVE STEPS: A KINETIC MODEL FOR THE REACTION

We have seen in Figure 4 (left) that the reaction rate decreased much faster than the limiting reactant concentration did, hence excluding a pseudo-first order behavior (even under a large excess of organic ligand with respect to the metal ion). Actually, the absorbance (λ_1) - absorbance (λ_2) plots correlating the absorbances at two different wavelengths during the course of the reaction (Figure 2) give us a clue on the kinetic model applicable to the present reaction, since their curvature indicates the involvement of at least a long-lived intermediate in the mechanism, not reactive enough to be in steady state, the slow step being thus the one corresponding to its decay:

$$\mathrm{R} \xrightarrow[\text{fast}]{k_1} \mathrm{I} \xrightarrow[\text{slow}]{k_2} \mathrm{P} \qquad (2)$$

where R, I and P stand for the limiting reactant (the metal ion), the long-lived intermediate and the reaction product, respectively.

The exact integrated solutions for the time dependences of the concentrations of these species (that can be consulted in many chemical kinetics textbooks[37]) are the following:

$$[\mathrm{R}] = [\mathrm{R}]_\mathrm{o}\, e^{-k_1 t} \qquad (3)$$

$$[\mathrm{I}] = \frac{k_1\,[\mathrm{R}]_\mathrm{o}}{k_2 - k_1}\,(e^{-k_1 t} - e^{-k_2 t}) \qquad (4)$$

$$[\mathrm{P}] = [\mathrm{R}]_\mathrm{o} - [\mathrm{R}] - [\mathrm{I}] \qquad (5)$$

The total absorbance of the reacting mixture at a certain wavelength can be deduced by application of the Beer-Lambert law to the three Cr(III) complexes involved (reactant, long-lived intermediate and product):

$$A_\lambda = (\varepsilon_{\mathrm{R},\lambda}\,[\mathrm{R}] + \varepsilon_{\mathrm{I},\lambda}\,[\mathrm{I}] + \varepsilon_{\mathrm{P},\lambda}\,[\mathrm{P}])\,l \qquad (6)$$

where $\varepsilon_{R,\lambda}$, $\varepsilon_{I,\lambda}$ and $\varepsilon_{P,\lambda}$ are the respective molar absorption coefficients and l = 1 cm is the optical path length. The values of $\varepsilon_{R,\lambda}$ and $\varepsilon_{P,\lambda}$ are related to the initial and final absorbances as:

$$\varepsilon_{R,\lambda} = \frac{A_{\lambda,0}}{[R]_o \, l} \quad (7)$$

$$\varepsilon_{P,\lambda} = \frac{A_{\lambda,\infty}}{[R]_o \, l} \quad (8)$$

having been considered in eq 8 that the final concentration of the product equals the initial concentration of the limiting reactant, once the latter species and the long-lived intermediate are both exhausted. Whereas the value of $A_{\lambda,\infty}$ could be obtained from the final absorbance reading (once the reacting mixture reached the equilibrium state), that of $A_{\lambda,0}$ was not experimentally accessible in a direct way because at t = 0 the reactants were still being mixed together.

A computer program has been written in BASIC language to perform the required calculations. In this program different values of four fitting parameters ($A_{\lambda,0}$, $\varepsilon_{I,\lambda}$, k_1 and k_2) were systematically varied until the best fit was found. This was defined as the one that minimized the average error given by:

$$E = \frac{\sum_{i=1}^{N} \left| A_{i,cal} - A_{i,exp} \right|}{N} \quad (9)$$

where $A_{i,cal}$ and $A_{i,exp}$ are the calculated and experimental values of the absorbance at different instants during the course of the reaction, respectively, and N is the number of absorbance-time couples of experimental data recorded for each kinetic run. The program so developed yielded a good concordance between the calculated and experimental absorbances. Depending on the experimental conditions, the average error spanned within the range $E = 3.40 \times 10^{-4}$ to 1.50×10^{-3}.

Furthermore, given that the Cr(III)-alanine reaction (under conditions of a large excess of organic ligand) has been previously reported in the chemical literature to follow a pseudo-first order behavior, it might be worth to compare the quality of the absorbance-time fits attained with two mathematical alternatives: the biparametric pseudo-first order kinetic model (involving $A_{\lambda,0}$ and k) and the tetraparametric model (involving $A_{\lambda,0}$, $\varepsilon_{I,\lambda}$, k_1 and k_2) used in the present

work. As can be seen in Figure 5, the ratio between the experimental and calculated absorbances during the course of the reaction was much closer to unity when the two rate constant kinetic model was employed.

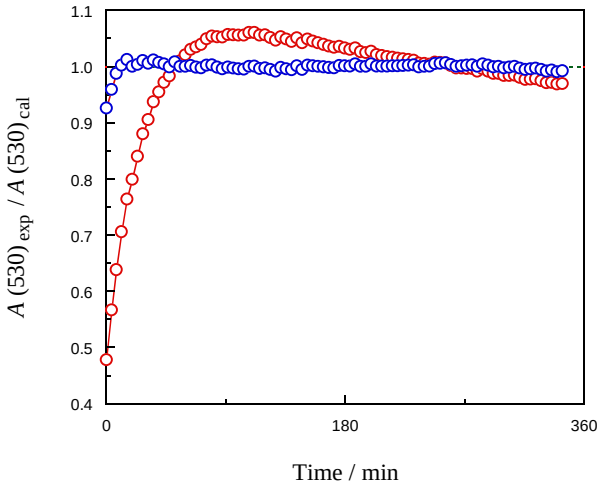

Figure 5. Ratio between the experimental and calculated absorbances at 530 nm as a function of time during the course of the reaction. Red: biparametric (pseudo-first order) kinetic model ($E = 9.17 \times 10^{-3}$). Blue: tetraparametric (two rate constant) kinetic model ($E = 7.30 \times 10^{-4}$). $[Cr(NO_3)_3]_o = 5.88 \times 10^{-3}$ M, [L-alanine]$_o$ = 0.133 M, $[KOH]_o = 8.28 \times 10^{-3}$ M, pH_∞ 3.97, 25.0 ºC.

The failure of the pseudo-first order model was rather notable during the whole reaction, but especially at its beginning, since there was an initial period where the calculated absorbances were systematically higher than their experimental counterparts (this deviation was greatly reduced in the case of the two rate constant model).

9. KINETIC RESULTS

The reaction rate is always a function of several variables. In the case of the Cr(III)-alanine complexation, the dependences of the rate on the initial concentrations of metal ion and ligand, ionic strength, pH and temperature are of special interest. In order to make easier the analysis of the results, it is the usual procedure in chemical kinetics to organize the experiments in several series, isolating one of the variables in each series and keeping all the others constant whenever possible. Because of its convenience, this method has been applied in the present study, and the results found are described hereafter.

9.1. EFFECT OF THE METAL ION INITIAL CONCENTRATION

A series of kinetic runs was performed at different Cr(III) initial concentrations, all the other experimental conditions remaining constant.

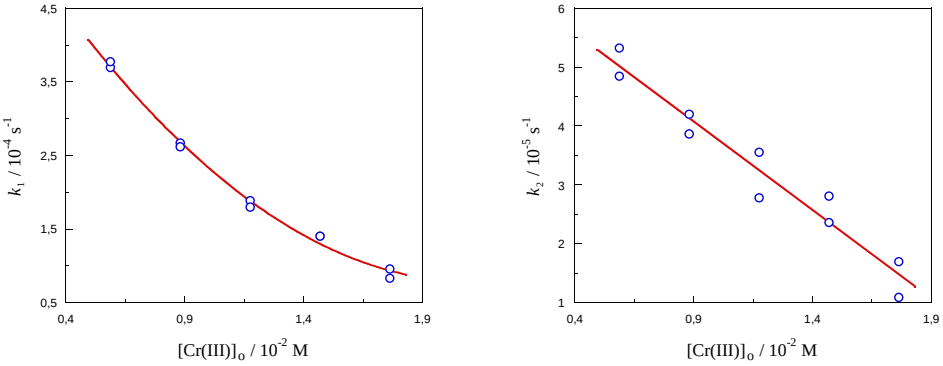

Figure 6. Dependence of experimental rate constants k_1 (left, r = 0.998) and k_2 (right, r = 0.972) on the initial concentration of metal ion. $[Cr(NO_3)_3]_o$ = (0.59 – 1.76) × 10^{-2} M, $[L\text{-alanine}]_o$ = 0.354 M, $[KOH]_o$ = 5.03 × 10^{-3} M, pH_∞ 3.72 – 4.12, 25.0 ºC.

Both rate constants decreased as the metal ion initial concentration increased, k_1 according to an upward-concave curve (Figure 6, left), whereas k_2 yielded a straight line (Figure 6, right). The decrease of the rate constants as the initial concentration of the limiting reactant increased was caused by the corresponding decrease in the reacting mixture initial pH (as we will see later, the reaction presents base catalysis). This rise in the medium acidity can be explained by the dissociation of hexaaquachromium(III) ion to yield hydroxopentaaquachromium(III) ion.[38,39]

9.2. EFFECT OF THE ORGANIC LIGAND INITIAL CONCENTRATION

In a series of kinetic experiments at gradually increasing initial concentration of L-alanine and constant concentration of KOH both rate constants increased. Their double-logarithm plots against the organic ligand initial concentration yielded straight lines with slopes 0.40 ± 0.03 in the case of k_1 (Figure 7, left) and 0.40 ± 0.02 in that of k_2 (Figure 7, right). This means that the apparent kinetic orders of the amino acid were fractional (non-integer) numbers, thus excluding the possibility of the reaction being of first order as far as the concentration of L-alanine was concerned.

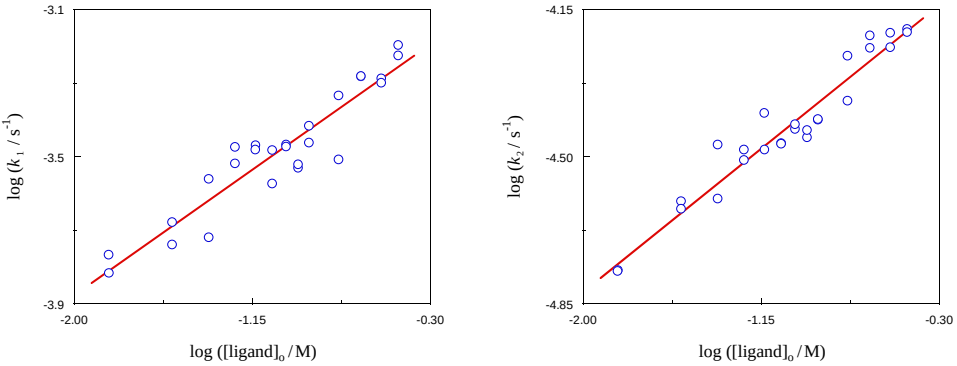

Figure 7. Double-logarithm plots showing the dependence of experimental rate constants k_1 (left, r = 0.938) and k_2 (right, r = 0. 969) on the initial concentration of L-alanine. $[Cr(NO_3)_3]_o$ = 5.88 × 10^{-3} M, [L-alanine]$_o$ = 0.015 – 0.354 M, $[KOH]_o$ = 8.28 × 10^{-3} M, pH_∞ 3.79 – 4.24, 25.0 ºC.

9.3. EFFECT OF THE IONIC STRENGTH

The ionic strength of the medium was changed by the use of KNO_3 as background electrolyte, and its effects on both experimental rate constants have been determined. A plot of the logarithm of each magnitude against $I^{1/2}/(1+I^{1/2})$ yielded straight lines with the slopes 0.93 ± 0.18 (for k_1, Figure 8, left) and - 0.43 ± 0.26 (for k_2, Figure 8, right) $M^{-1/2}$.

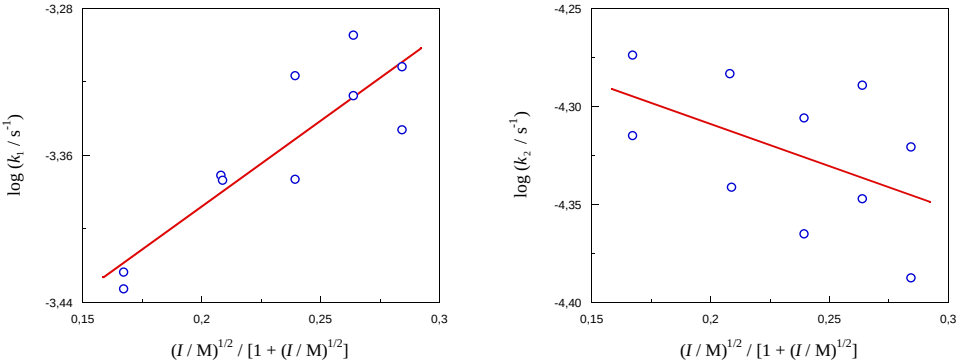

Figure 8. Dependence of experimental rate constants k_1 (left, r = 0.876) and k_2 (right, r = 0. 507) on the medium ionic strength. $[Cr(NO_3)_3]_o$ = 5.88 × 10^{-3} M, $[L\text{-alanine}]_o$ = 0.354 M, $[KOH]_o$ = 5.03 × 10^{-3} M, $[KNO_3]$ = 0.000 – 0.118 M, pH_∞ 4.12 – 4.20, 25.0 ºC.

9.4. Effect of the pH

The pH of the medium was varied by means of a changing concentration of KOH. An increase of the pH resulted in an increase of both k_1 (Figure 9, left) and k_2 (Figure 9, right), indicating the existence of base catalysis in the two cases.

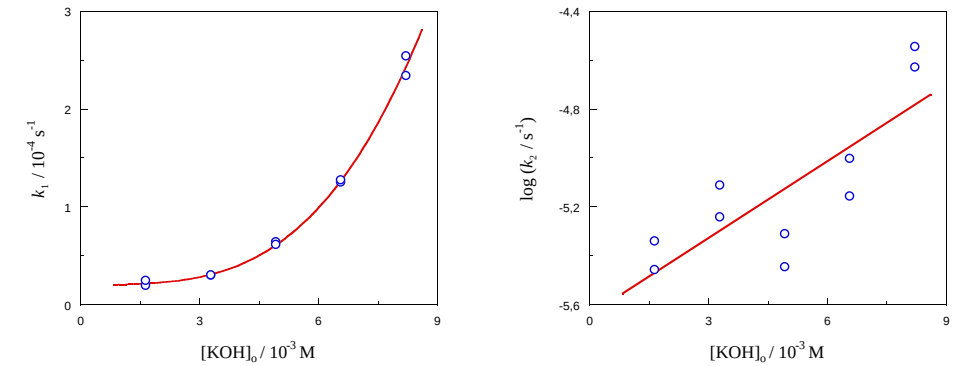

Figure 9. Dependence of experimental rate constants k_1 (left, r = 0.999) and k_2 (right, r = 0. 808) on the initial concentration of potassium hydroxide. $[Cr(NO_3)_3]_o$ = 5.88 × 10^{-3} M, $[L\text{-alanine}]_o$ = 5.89 × 10^{-2} M, $[KOH]_o$ = (1.64 – 8.21) × 10^{-3} M, pH_∞ 3.56 – 3.84, 25.0 ºC.

9.5. EFFECT OF TEMPERATURE

Both experimental rate constants increased with increasing temperature in the range 20.0-30.0 ºC. The rate constant vs. temperature data were fitted by least squares to the linearized forms of either the Arrhenius equation:

$$k = A\, e^{-\frac{E_a}{RT}} \qquad (10)$$

where A is the pre-exponential factor, E_a the activation energy, R the gas constant and T the absolute temperature, or, alternatively, the Eyring equation:

$$k = \kappa \frac{k_B T}{h} (c^o)^{1-n}\, e^{\frac{\Delta S^o_{\neq}}{R}}\, e^{-\frac{\Delta H^o_{\neq}}{RT}} \qquad (11)$$

k_B and h being respectively the Boltzmann and Plank constants, c^o the standard concentration (1 mol L^{-1}), $\Delta S^o_{\neq}$ the activation entropy and $\Delta H^o_{\neq}$ the activation enthalpy. Parameter κ is the transmission coefficient (the probability of the activated complex breaking down into the reaction products) and it is usually taken as unity, given our lack of knowledge about its value. Equation 11 was originally written without the standard concentration factor, but it was introduced later to assure its dimensional homogeneity.[40]

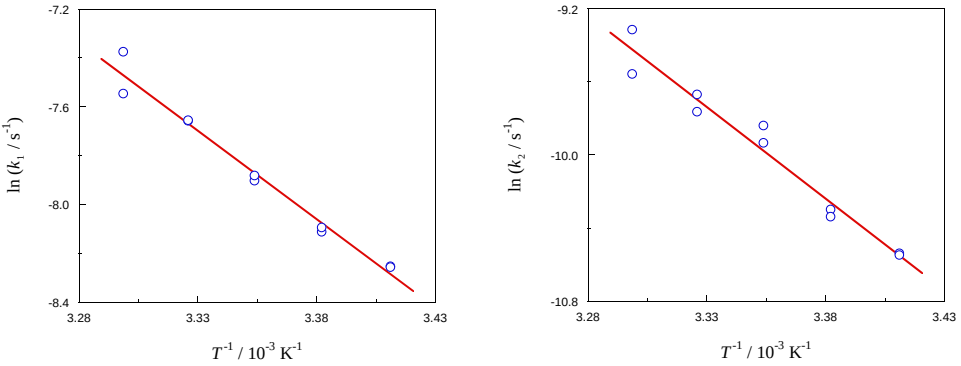

Figure 10. Dependence of experimental rate constants k_1 (left, r = 0.988) and k_2 (right, r = 0. 981) on the temperature. $[Cr(NO_3)_3]_o$ = 5.88 × 10^{-3} M, $[L\text{-alanine}]_o$ = 0.354 M, $[KOH]_o$ = 5.03 × 10^{-3} M, pH_∞ 4.06 ± 0.03, 20.0 – 30.0 ºC.

The linearized Arrhenius plots for rate constants k_1 (Figure 10, left) and k_2 (Figure 10, right) are shown above, whereas the corresponding parameters (as well as those associated with the Eyring plots) are compiled in Table 1.

Rate constant	ln *A*	E_a [kJ mol^{-1}]	$\Delta H^{o}_{\neq}$ [kJ mol^{-1}]	$\Delta S^{o}_{\neq}$ [J K^{-1} mol^{-1}]
k_1	16.4 ± 1.3	60.2 ± 3.3	57.7 ± 3.3	- 116.8 ± 11.0
k_2	23.6 ± 2.4	83.3 ± 5.9	80.9 ± 5.9	- 56.6 ± 19.7

(a) The errors associated with the Arrhenius and Eyring magnitudes were calculated from the standard deviations for the intercepts and slopes of the corresponding plots.

Table 1. Arrhenius and Eyring magnitudes associated with the experimental rate constants. $[Cr(NO_3)_3]_o$ = 5.88 × 10^{-3} M, $[\text{L-alanine}]_o$ = 0.354 M, $[KOH]_o$ = 5.03 × 10^{-3} M, pH_∞ 4.06 ± 0.03, 20.0 – 30.0 ºC.

It should be noticed, however, that the parameter values given in Table 1 must be considered as only apparent, because of their dependences on both the amino acid concentration and pH.

10. CONCERNING THE LONG-LIVED INTERMEDIATE

The UV-Vis spectrum of the intermediate present in non-steady state conditions could not be directly recorded, given that in any moment during the course of the reaction it was always in a mixture with the reactant and the product (the three of them absorbing light). Fortunately, however, it was possible to calculate the molar absorption coefficient of that intermediate at each wavelength. For that purpose, we started with the localization of the instant at which the long-lived intermediate reached its maximum concentration, as well as the concentrations of the three species at that instant (from eqs 3 – 5):

$$t_{\max} = \frac{1}{k_1 - k_2} \ln \frac{k_1}{k_2} \qquad [R]_{\max} = [R]_o \, e^{-k_1 t_{\max}} \tag{12}$$

$$[I]_{\max} = \frac{k_1}{k_2} [R]_o \, e^{-k_1 t_{\max}} \qquad [P]_{\max} = [R]_o - [R]_{\max} - [I]_{\max} \tag{13}$$

Then, from the periodic scanning of the UV-Vis spectra during the course of the reaction (Figure 1), an interpolation between the two intermediary spectra closer to t_{max} led to the spectrum of the reacting mixture at the exact moment when the long-lived intermediate presented its maximum concentration, and the spectrum of the latter could be obtained by discounting from the total absorbance (A_λ) the contributions of the other two chemical species absorbing light:

$$\varepsilon_{I,\lambda} = \frac{A_\lambda - (\varepsilon_{R,\lambda}\,[R]_{max} + \varepsilon_{P,\lambda}\,[P]_{max})\,l}{[I]_{max}\,l} \qquad (14)$$

It can be observed (Figure 11) that the spectra of the reactant, intermediate and product all exhibit two peaks, both the wavelengths and intensities for the long-lived intermediate being intermediary between those corresponding to the reactant and product.

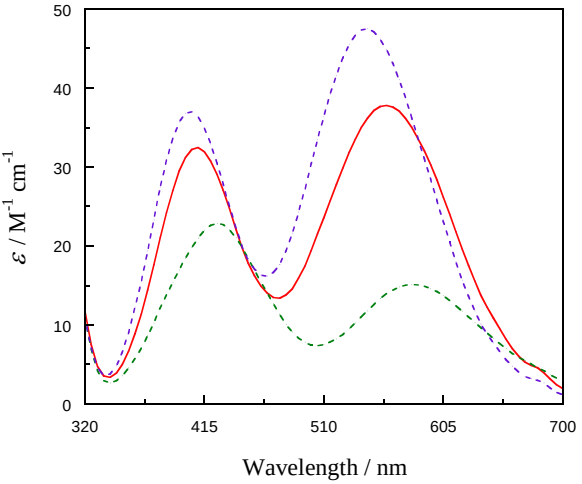

Figure 11. Molar absorption coefficients as a function of the wavelength for three Cr(III) complexes: reactant (green dashed line), long-lived intermediate (red continuous line) and final product (violet dashed line). $[Cr(NO_3)_3]_o$ = 1.76 × 10^{-2} M, [L-alanine]$_o$ = 0.354 M, $[KOH]_o$ = 5.03 × 10^{-3} M, pH_∞ 3.71, 25.0 ºC.

11. CONCERNING THE REACTION PRODUCTS

11.1. NUMBER OF RELEASED HYDROGEN IONS

Under the experimental conditions of the present work, the amino acid was present chiefly in its zwitterionic form, involving a protonated amino group and an anionic carboxylate group. Consequently, in order to coordinate itself with the metal ion, it can be anticipated that the organic ligand must undergo the loss of a hydrogen ion from the ammonium group, so that the free nitrogen atom can behave as an electron-pair donor to the metal acting as a Lewis acid.

Actually, the number of hydrogen ions released to the medium per chromium atom during the reaction can be calculated from the value of pH_∞ by means of the following equation:

$$\text{Number}\,(H^+) = \left\{\left(\frac{[L]_o - n\,[M]_o}{K_a + [H^+]_\infty} + 1\right)[H^+]_\infty + [B]_o\right\}\frac{1}{[M]_o} \qquad (15)$$

where L, B and M stand for ligand, base (potassium hydroxide) and metal, respectively, n is the number of organic ligands coordinated per chromium atom and K_a is the first acid-dissociation equilibrium constant of protonated L-alanine (for the carboxyl group, pK_a 2.35 at 25.0 ºC).[41,42]

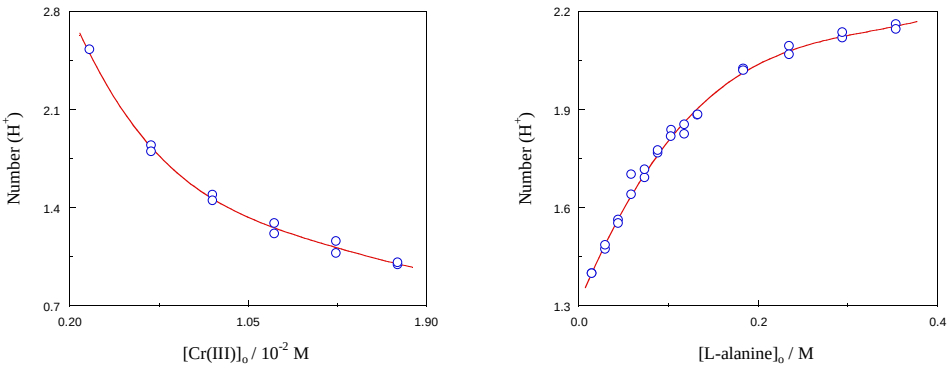

Figure 12. Dependence of the number of hydrogen ions released per chromium atom on the initial concentrations of the reactants at 25.0 ºC. Left: $[Cr(NO_3)_3]_o$ = (0.29 – 1.76) × 10^{-2} M, $[L\text{-alanine}]_o$ = 0.354 M, $[KOH]_o$ = 5.03 × 10^{-3} M, pH_∞ 3.72 – 4.12. Right: $[Cr(NO_3)_3]_o$ = 5.88 × 10^{-3} M, $[L\text{-alanine}]_o$ = 0.015 – 0.354 M, $[KOH]_o$ = 8.28 × 10^{-3} M, pH_∞ 3.84 – 4.25.

The number of hydrogen ions so calculated decreased as the initial concentration of Cr(III) increased (Figure 12, left), and increased as those of either amino acid (Figure 12, right) or potassium hydroxide (Figure 13) increased, remaining always within the range 0.73 – 2.53.

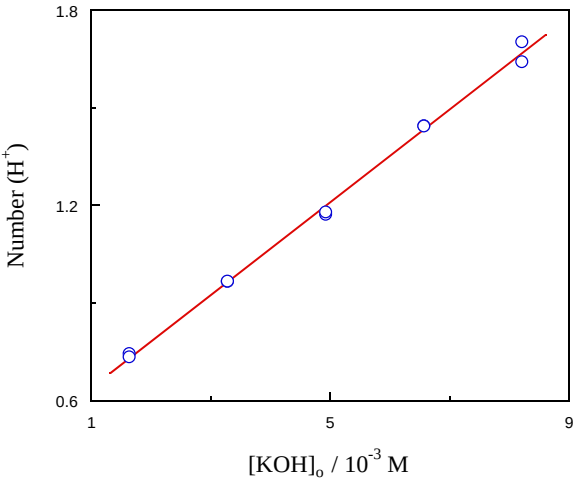

Figure 13. Dependence of the number of hydrogen ions released per chromium atom on the initial concentration of potassium hydroxide. $[Cr(NO_3)_3]_o = 5.88 \times 10^{-3}$ M, $[L\text{-alanine}]_o = 5.89 \times 10^{-2}$ M, $[KOH]_o = (1.64 - 8.21) \times 10^{-3}$ M, pH 3.55 – 3.84, 25.0 ºC.

11.2. UV-VIS SPECTRA OF THE CHROMIUM(III)-ALANINE COMPLEXES

The final reaction mixture showed a distinct violet color and, once recorded its UV-Vis spectrum, two peaks at 405 (lower intensity) and 543 (higher intensity) nm were observed (Figure 14). However, an increase of the Cr(III) initial concentration resulted in a shift of the two absorption peaks recorded for the final violet complex toward higher wavelengths (Figure 15, bottom). As could be easily anticipated, the corresponding maximum absorbances increased indeed, but the plots were not linear, showing a downward-concave curvature instead (Figure 15, top). In fact, even if the wavelength was kept constant (530 nm), there was a clear-cut unfulfillment of the Lambert-Beer law, since the molar absorption coefficient decreased as the metal ion initial concentration increased (Figure 16).

On the contrary, an increase of the L-alanine initial concentration resulted in a shift of the two spectral absorption peaks for the final violet complex toward lower wavelengths (Figure 17, bottom).

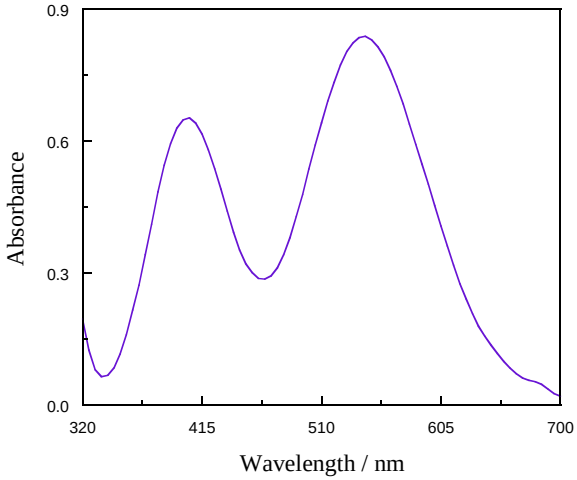

Figure 14. UV-Vis spectrum of the final reaction mixture. $[Cr(NO_3)_3]_o$ = 1.76 × 10^{-2} M, $[L\text{-alanine}]_o$ = 0.354 M, $[KOH]_o$ = 5.03 × 10^{-3} M, pH_∞ 3.71, 25.0 ºC.

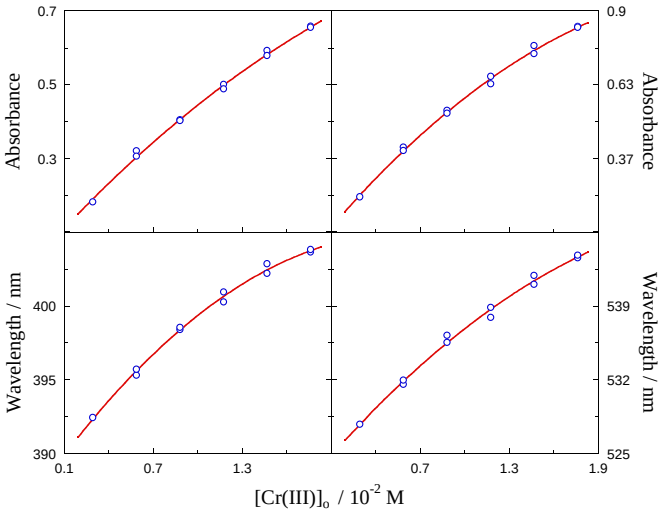

Figure 15. Wavelengths (bottom) and absorbances (top) corresponding to the first (left) and second (right) peaks of the electronic spectrum recorded for the final violet complex as a function of the metal ion initial concentration. $[Cr(NO_3)_3]_o$ = (0.29 – 1.76) × 10^{-2} M, $[L\text{-alanine}]_o$ = 0.354 M, $[KOH]_o$ = 5.03 × 10^{-3} M, pH_∞ 3.72 – 4.12, 25.0 ºC.

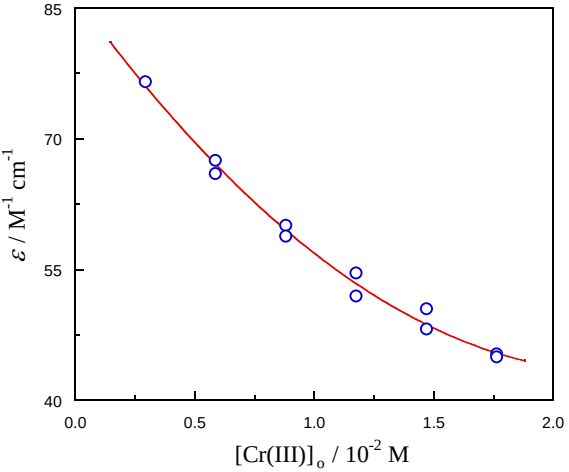

Figure 16. Molar absorption coefficient at 530 nm as a function of the limiting reactant initial concentration. $[Cr(NO_3)_3]_o$ = (0.29 – 1.76) × 10^{-2} M, $[L\text{-alanine}]_o$ = 0.354 M, $[KOH]_o$ = 5.03 × 10^{-3} M, pH_∞ 3.72 – 4.12, 25.0 °C.

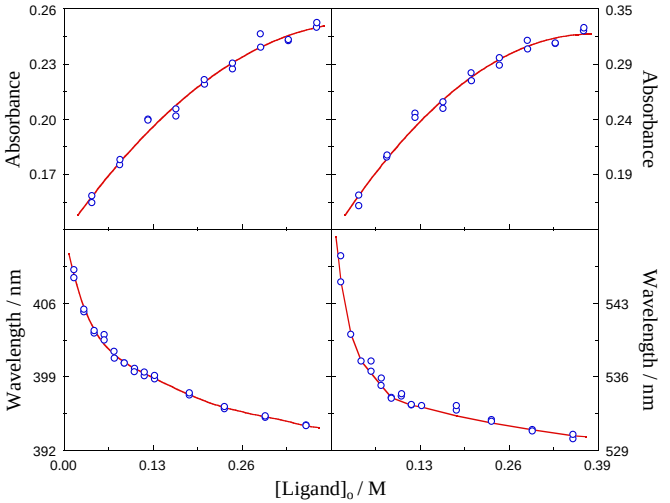

Figure 17. Wavelengths (bottom) and absorbances (top) corresponding to the first (left) and second (right) peaks of the electronic spectrum recorded for the final violet complex as a function of the organic ligand initial concentration. $[Cr(NO_3)_3]_o$ = 5.88 × 10^{-3} M, $[L\text{-alanine}]_o$ = 0.015 – 0.354 M, $[KOH]_o$ = 8.28 × 10^{-3} M, pH_∞ 3.84 – 4.25, 25.0 °C.

As observed before for the effect of the metal ion initial concentration, the corresponding maximum absorbances increased, but the plots were not linear either, showing a downward-concave curvature again (Figure 17, top).

The wavelengths and molar absorption coefficients for the first and second peaks of the UV-Vis (electronic) spectra recorded for the final (violet) reaction product could be fitted to functions of the types:

$$\lambda = \frac{a_\lambda + b_\lambda [\mathrm{X}]_o}{1 + c_\lambda [\mathrm{X}]_o} \quad (16)$$

$$\varepsilon = \frac{a_\varepsilon + b_\varepsilon [\mathrm{X}]_o}{1 + c_\varepsilon [\mathrm{X}]_o} \quad (17)$$

where X = Cr(III) or L-alanine. In order to obtain the values of the parameters associated with the electronic spectra corresponding to the reactant (with zero organic ligands) and product (with the highest possible number of organic ligands), under the experimental conditions of our study, extrapolations at $[X]_o = 0$ and ∞ were performed:

$$\lim_{[X]_o \to 0} \lambda = a_\lambda \qquad \lim_{[X]_o \to \infty} \lambda = \frac{b_\lambda}{c_\lambda} \quad (18)$$

$$\lim_{[X]_o \to 0} \varepsilon = a_\varepsilon \qquad \lim_{[X]_o \to \infty} \varepsilon = \frac{b_\varepsilon}{c_\varepsilon} \quad (19)$$

X	λ_R	λ_P	ε_R	ε_P
Cr(III)	b_λ / c_λ	a_λ	$b_\varepsilon / c_\varepsilon$	a_ε
L-Ala	a_λ	b_λ / c_λ	a_ε	$b_\varepsilon / c_\varepsilon$

(a) L-Ala stands for L-alanine.

Table 2. Correspondence between the wavelengths and molar absorption coefficients associated with the UV-Vis peaks of the green (reactant, R) and violet (product, P) complexes and the fitting parameters appearing in eqs 16 and 17.

In this way, the parameters belonging to the spectrum of the reactant could be deduced from the extrapolations at either $[\text{L-alanine}]_o = 0$ or $[\text{Cr(III)}]_o = \infty$, whereas those for the product were inferred from the extrapolations at either $[\text{Cr(III)}]_o = 0$ or $[\text{L-alanine}]_o = \infty$ (Table 2).

The extrapolated values so obtained appear compiled in Table 3. It should be noticed that the ones obtained at infinite initial concentrations (of either metal ion or amino acid) are to be preferred over those obtained at zero initial concentrations, for they are closer to the experimental values in the case of the reactant (the only species for which the spectrum parameters are directly accessible).

Peak parameter	Reactant	Product
λ_1 [nm]	421 (412)	391 (388)
λ_2 [nm]	581 (564)	530 (522)
ε_1 [M^{-1} cm^{-1}]	22.2 (23.3)	70.4 (82.0)
ε_2 [M^{-1} cm^{-1}]	12.2 (19.2)	83.4 (89.4)

(a) The main values were obtained by extrapolation at infinite initial concentrations of either metal ion(reactant) or amino acid (product).
(b) The values in parenthesis were obtained by extrapolation at zero initial concentrations of either metal ion (product) or amino acid (reactant).
(c) Changing the metal ion initial concentration: $[Cr(NO_3)_3]_o = (0.29 - 1.76) \times 10^{-2}$ M, $[\text{L-alanine}]_o = 0.354$ M, $[KOH]_o = 5.03 \times 10^{-3}$ M, pH∞ 3.72 - 4.12.
(d) Changing the amino acid initial concentration: $[Cr(NO_3)_3]_o = 5.88 \times 10^{-3}$ M, $[\text{L-alanine}]_o = 0.015 - 0.354$ M, $[KOH]_o = 8.28 \times 10^{-3}$ M, pH∞ 3.84 - 4.25.

Table 3. Values of the wavelengths and molar absorption coefficients associated with the first and second UV-Vis peaks of the green (reactant) and violet (product) complexes at 25.0 ºC.

A variation of the initial potassium hydroxide concentration had also an effect on the UV-Vis spectrum of the reaction product mixture. As can be observed, an increase of the initial base concentration resulted in a decrease of the wavelengths associated with the two peaks (Figure 18, bottom) and an increase of the corresponding absorbances (Figure 18, top).

The spectroscopic data shown in Figures 15, 17 and 18 indicate that the wavelength for the first visible peak of the final reacting mixture lied in the range 392 – 409 nm, and for the second in the range 528 – 548 nm, increasing both with the initial concentration of metal ion and decreasing both with the initial concentrations of either ligand or potassium hydroxide.

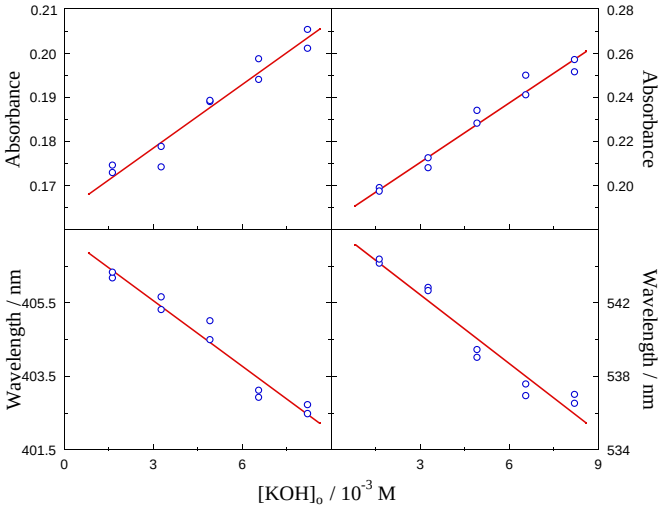

Figure 18. Wavelengths (bottom) and absorbances (top) corresponding to the first (left) and second (right) peaks of the electronic spectrum recorded for the final violet complex as a function of the potassium hydroxide initial concentration. $[Cr(NO_3)_3]_o = 5.88 \times 10^{-3}$ M, $[\text{L-alanine}]_o = 5.89 \times 10^{-2}$ M, $[KOH]_o = (1.64 - 8.21) \times 10^{-3}$ M, pH 3.55 – 3.84, 25.0 °C.

The values reported for the number of organic ligands coordinated to Cr(III) in the final violet complex depend on the bibliographic source consulted, the stoichiometric ratio for metal ion : organic ligand being 1 : 2 for some authors[30] and 1 : 3 for others.[29] Actually, the results shown in Figures 15-18 cannot be explained unless we assume the presence of at least four different complexes in the final reacting mixture. Thus, although the participation of other complexes cannot be discarded, the simplest explanation for the experimental data so far available is that four complexes differing either in the number of organic ligands or in their acid-base properties coexist in equilibrium in the final reacting mixture:

$$C_n - H^+ + \text{Ala} \underset{}{\overset{K_1}{\rightleftharpoons}} C_{n+1} - H^+ \qquad (20)$$

$$C_n + \text{Ala} \underset{}{\overset{K_2}{\rightleftharpoons}} C_{n+1} \qquad (21)$$

where C_n (or C_n–H^+) and C_{n+1} (or C_{n+1}–H^+) are Cr(III) complexes involving n and $n+1$ L-alanine ligands, respectively, their total concentrations being $[C_n]_T = [C_n] + [C_n–H^+]$ and $[C_{n+1}]_T = [C_{n+1}] + [C_{n+1}–H^+]$. From a mass balance, it follows that:

$$\frac{[C_{n+1} - H^+]}{[C_n - H^+]} = K_1 \left\{[Ala]_T - n[C_n]_T - (n+1)[C_{n+1}]_T\right\} \quad (22)$$

$$\frac{[C_{n+1}]}{[C_n]} = K_2 \left\{[Ala]_T - n[C_n]_T - (n+1)[C_{n+1}]_T\right\} \quad (23)$$

Since an increase of the metal ion initial concentration results in an increase of the total concentrations of both complexes C_n and C_{n+1}, and so in a decrease of the $[C_{n+1}\text{-}H^+]/[C_n\text{-}H^+]$ and $[C_{n+1}]/[C_n]$ ratios, whereas an increase of the L-alanine initial concentration leads to the opposite result (an increase of the $[C_{n+1}\text{-}H^+]/[C_n\text{-}H^+]$ and $[C_{n+1}]/[C_n]$ ratios), eqs 22 and 23 are consistent with the plots shown in Figures 15-17 provided that the electronic spectra corresponding to the different complexes are shifted toward lower wavelengths as the number of organic ligands increases and, at the same time, there is an enhancement of the intensity of the absorption peaks:

$$\lambda_{1,2}(0) > \lambda_{1,2}(n) > \lambda_{1,2}(n+1) \quad (24)$$

$$\varepsilon_{1,2}(0) < \varepsilon_{1,2}(n) < \varepsilon_{1,2}(n+1) \quad (25)$$

In the inequalities written in eqs 24 and 25 the subscripts indicate that the wavelengths and molar absorption coefficients correspond to both peaks of the spectrum (the first and the second), and the quantities within parentheses stand for the number of organic ligands involved in each of the five complexes proposed: 0 for the initial green complex, n for the final violet complexes $C_n\text{-}H^+$ or C_n, and $n+1$ for the final violet complexes $C_{n+1}\text{-}H^+$ or C_{n+1}.

In addition, the finding of a clear-cut dependence of the electronic spectrum of the final reacting mixture on the pH of the medium (Figure 18) allows us to infer that:

$$\lambda_{1,2}(C_n) < \lambda_{1,2}(C_n - H^+) \quad (26)$$

$$\lambda_{1,2}(C_{n+1}) < \lambda_{1,2}(C_{n+1} - H^+) \quad (27)$$

$$\varepsilon_{1,2}(C_n) > \varepsilon_{1,2}(C_n - H^+) \quad (28)$$

$$\varepsilon_{1,2}(C_{n+1}) > \varepsilon_{1,2}(C_{n+1} - H^+) \quad (29)$$

12. A MICROSCOPIC LOOK AT THE REACTION

12.1. CHROMIUM(III) SPECIATION: CONCENTRATION-pH PLOTS

The kinetics of the reaction between Cr(III) and L-alanine resembles that of other similar processes, such as the complexations of the same metal ion by EDTA[5] or the α-amino acids L-glutamic acid,[26] DL-leucine[25] and DL-lysine,[26] in that all of them exhibit base catalysis. It is precisely this pH dependence that offers the main clue to elucidate the mechanism involved in the reaction.

Trivalent chromium finds itself in slightly acidic aqueous solutions in the form of several species in equilibrium, from hexaaquachromium(III) ion to dissolved (either monomolecular or colloidal) chromium(III) hydroxide, passing through the monohydroxo and dihydroxo complexes:

$$[Cr(H_2O)_6]^{3+} \xrightleftharpoons{K_I} [Cr(OH)(H_2O)_5]^{2+} + H^+ \quad (30)$$

$$[Cr(OH)(H_2O)_5]^{2+} \xrightleftharpoons{K_{II}} [Cr(OH)_2(H_2O)_4]^{+} + H^+ \quad (31)$$

$$[Cr(OH)_2(H_2O)_4]^{+} \xrightleftharpoons{K_{III}} [Cr(OH)_3(H_2O)_3] + H^+ \quad (32)$$

Although the corresponding equilibrium constants were not known with exactitude for some time,[43] a recent publication has reported experimental values for them that can be considered as reliable ($pK_{a,1}$ 3.52, $pK_{a,2}$ 5.78, $pK_{a,3}$ 7.88).[44]

Since, according to the kinetic model developed in the present work, rate constant k_1 should be considered as the ratio between the initial values of the reaction rate and the concentration of the inorganic (limiting) reactant, it must be correlated with the initial pH of the reacting mixtures. Unfortunately, given the slow response of the pH meter to yield accurate measurements, the only pH data experimentally accessible with a high degree of confidence are those corresponding to an equilibrium state (pH_∞). However, the initial pH for each kinetic run could be theoretically calculated from the first (eq 30) and second (eq 31) acid-dissociation equilibrium constants of hexaaquachromium(III) ion[44] and the first of the protonated form of L-alanine (pK_a 2.35 at 25.0 ºC)[41,42] following the mathematical formula:

$$pH_o = -\log \frac{-b + \sqrt{b^2 + 4ac}}{2a} \qquad (33)$$

where the parameters required to solve the involved quadratic equation depend on which chemical species was initially in excess (either the metal ion or potassium hydroxide) and appear compiled in Table 4.

Conditions	*a*	*b*	*c*
$[B]_o < [M]_o$	$1 + [L]_o / K_a$	$K_I(1 + [L]_o / K_a) + [B]_o$	$K_I([M]_o - [B]_o)$
$[B]_o > [M]_o$	$1 + [L]_o / K_a$	$K_{II}(1 + [L]_o / K_a) + [B]_o - [M]_o$	$K_{II}(2[M]_o - [B]_o)$

(a) B, M and L stand for base (potassium hydroxide), metal and organic ligand, respectively.

(b) K_a, K_I and K_{II} stand for the acid-dissociation equilibrium constants of the protonated form of L-alanine (first) and hexaaquachromium(III) ion (first and second), respectively.

Table 4. Values of the parameters required to calculate the initial pH depending on the experimental conditions.

The correspondence between the initial (calculated from eq 33) and final (measured) pH values for the series of kinetic runs performed at different potassium hydroxide initial concentrations is shown in Figure 19. We can observe that the pH decrease due to the release of hydrogen ions during the reaction increased dramatically as $[KOH]_o$ increased. It should be noticed that the use of a buffer was not advised because of the potential competition between the anionic basic form of the buffer and L-alanine as ligands for the metal ion.

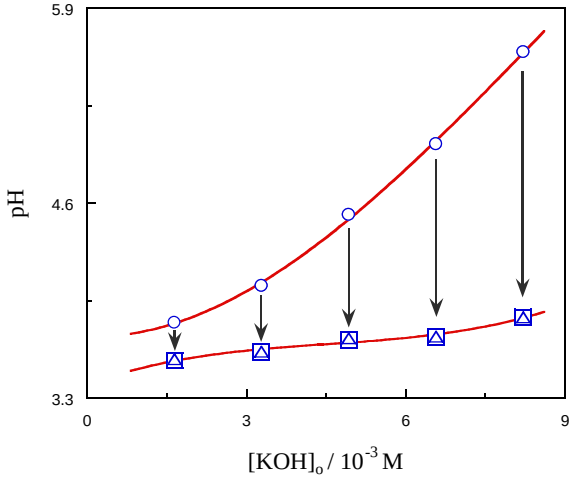

Figure 19. Correspondence between the initial (calculated, circles) and final (experimental, squares and triangles) values of the pH at different potassium hydroxide initial concentrations. The arrows indicate the change of pH during the kinetic runs. $[Cr(NO_3)_3]_o$ = 5.88 × 10^{-3} M, $[L\text{-alanine}]_o$ = 5.89 × 10^{-2} M, $[KOH]_o$ = (1.64 – 8.21) × 10^{-3} M, pH_∞ 3.56 – 3.84, 25.0 ºC.

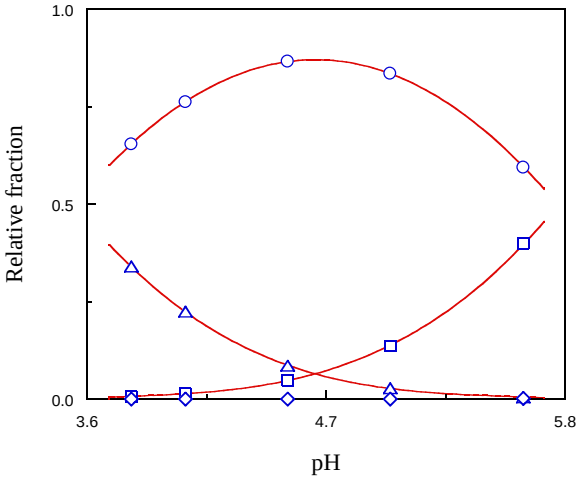

Figure 20. Relative fractions of $[Cr(H_2O)_6]^{3+}$ (triangles), $[Cr(OH)(H_2O)_5]^{2+}$ (circles), $[Cr(OH)_2(H_2O)_4]^{+}$ (squares) and $Cr(OH)_3$ (rhombuses) as a function of pH at 25.0 ºC.

The relative fractions of the different Cr(III) species present in equilibrium within the initial pH range covered by our kinetic experiments are shown in Figure 20. The predominant form was the monohydroxo complex, with appreciable amounts of both the hexaaqua and dihydroxo complexes, and the hydroxide in negligible proportion.

In a first trial, we have attempted to calculate the value of experimental rate constant k_1 as a linear combination of the contributions of the four possible Cr(III) species:

$$k_{1,\mathrm{cal}} = \frac{\sum_{x=0}^{3} k_{1,x}\,[\mathrm{Cr(OH)_x(H_2O)_{6-x}}^{(3-x)+}]}{\sum_{x=0}^{3} [\mathrm{Cr(OH)_x(H_2O)_{6-x}}^{(3-x)+}]} \qquad (34)$$

A BASIC program was developed in order to find the best set of values $k_{1,x}$ ($x = 0 - 3$) minimizing the difference between the calculated ($k_{1,\mathrm{cal}}$) and experimental ($k_{1,\mathrm{exp}}$) rate constants. However, a $k_{1,\mathrm{exp}}$ vs. $k_{1,\mathrm{cal}}$ plot yielded a downward-concave curve (Figure 21, left).

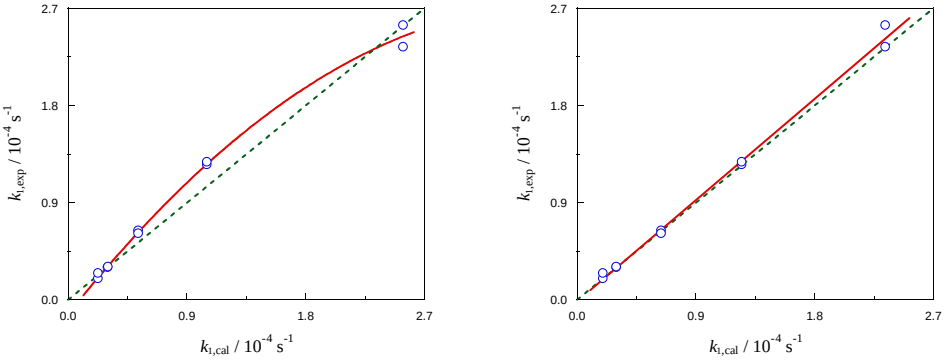

Figure 21. Correspondence between the experimental values of the first rate constant and those calculated according to either eq 34 (left) or eq 35 (right). The dashed lines correspond to a perfect concordance between $k_{1,\mathrm{exp}}$ and $k_{1,\mathrm{cal}}$. $[Cr(NO_3)_3]_o$ = 5.88 × 10^{-3} M, $[L\text{-alanine}]_o$ = 5.89 × 10^{-2} M, $[KOH]_o$ = (1.64 – 8.21) × 10^{-3} M, pH_∞ 3.56 – 3.84, 25.0 °C.

Therefore, a second trial was made (considering now negligible the contribution corresponding to $x = 0$) with a function of the type:

$$k_{1,\mathrm{cal}} = \frac{[\mathrm{H}^+]_o}{1 + K[\mathrm{H}^+]_o} \frac{\sum_{x=1}^{3} k_{1,x}[\mathrm{Cr(OH)_x(H_2O)_{6-x}}^{(3-x)+}]}{\sum_{x=1}^{3}[\mathrm{Cr(OH)_x(H_2O)_{6-x}}^{(3-x)+}]} \quad (35)$$

yielding the results $k_{1,1}$ = 1.77 M^{-1} s^{-1}, $k_{1,2}$ = 128 M^{-1} s^{-1}, $k_{1,3}$ = 3.07 × 10^4 M^{-1} s^{-1} and K = 9.66 × 10^4 M^{-1}, with an excellent concordance between $k_{1,\mathrm{cal}}$ and $k_{1,\mathrm{exp}}$ (Figure 21, right). We can see that, according to these data, the reactivity of the chromium species toward L-alanine increases following the sequence $\mathrm{CrOH^{2+}} < \mathrm{Cr(OH)_2^+} < \mathrm{Cr(OH)_3}$, each time an aqua ligand is replaced by a hydroxo ligand resulting in a rate constant enhancement by two orders of magnitude.

12.2. MECHANISM

According to the available experimental data, the mechanism that can be proposed for the complexation of Cr(III) by L-alanine consists of two elementary step sequences. The first leads from the reactants to the long-lived intermediate:

$$\mathrm{[Cr(OH)_x(H_2O)_{6-x}]^{(3-x)+}} \xrightarrow[\text{slow}]{k_{\mathrm{IV},x}} \mathrm{[Cr(OH)_x(H_2O)_{5-x}]^{(3-x)+}} + \mathrm{H_2O} \quad (36)$$

$$\mathrm{[Cr(OH)_x(H_2O)_{5-x}]^{(3-x)+}} + \mathrm{OH^-} \xrightarrow{k_{\mathrm{V},x}} \mathrm{[Cr(OH)_{x+1}(H_2O)_{5-x}]^{(2-x)+}} \quad (37)$$

$$\mathrm{[Cr(OH)_x(H_2O)_{5-x}]^{(3-x)+}} + \mathrm{H_2O} \xrightarrow{k_{\mathrm{VI},x}} \mathrm{[Cr(OH)_x(H_2O)_{6-x}]^{(3-x)+}} \quad (38)$$

$$\mathrm{[Cr(OH)_x(H_2O)_{5-x}]^{(3-x)+}} + \mathrm{RH} \xrightarrow{k_{\mathrm{VII},x}} \mathrm{[Cr(OH)_x(RH)(H_2O)_{5-x}]^{(3-x)+}} \quad (39)$$

$$\mathrm{[Cr(OH)_x(RH)(H_2O)_{5-x}]^{(3-x)+}} \longrightarrow \mathrm{[Cr(OH)_{x-1}(R)(H_2O)_{5-x}]^{(3-x)+}} + \mathrm{H_2O} \quad (40)$$

where x = 1, 2 or 3, depending on the particular reacting Cr(III) species, and RH stands for the zwitterionic form of the amino acid. The experimental results suggest that the presence of $\mathrm{OH^-}$ ligands in the reactant complex renders the Cr(III)-H_2O chemical bonds more labile. The

breakage of one of those bonds (as in eq 36) has been postulated to be a requirement for the formation of the Cr(III)-EDTA complex.[7] Then, a competition between hydroxide ion (eq 37), water (eq 38) and the organic ligand (eq 39) for the vacant coordination site of the metal ion takes place. In the last reaction the organic ligand suffers a conversion from monodentate to bidentate and a water molecule is released, leading to the formation of the long-lived intermediate (eq 40).

Assuming that the penta-coordinated intermediate is reactive enough to be in steady state (in other words, that it is formed in the slow step), the following expressions can be obtained for the parameters appearing in eq 35:

$$K = \frac{k_{\mathrm{VI,X}} + k_{\mathrm{VII,X}}\,[\mathrm{RH}]}{K_{\mathrm{W}}\,k_{\mathrm{V,X}}} \tag{41}$$

$$k_{1,\mathrm{X}} = \frac{k_{\mathrm{IV,X}}\,k_{\mathrm{VII,X}}}{K_{\mathrm{W}}\,k_{\mathrm{V,X}}}\,[\mathrm{RH}] \tag{42}$$

where K_{w} is the water ionic product. Equations 35, 41 and 42 are consistent with the dependence of k_1 on the initial concentration of organic ligand (fractional kinetic order, Figure 7, left). Moreover, the increasing effect of the ionic strength (Figure 8, left) can be explained by the decrease of rate constant $k_{\mathrm{V,X}}$, since eq 37 involves two unlike-charged ions as reactants (for x = 1 or 2), and the observed base catalysis (Figure 9, left) comes straightforward from the increase of $k_{\mathrm{IV,X}}$ as x increases from 1 to 3.

The second sequence (that parallels the first one) leads from the long-lived intermediate to the reaction products:

$$[\mathrm{Cr(OH)_{X-1}(R)(H_2O)_{5-X}}]^{(3-X)+} \xrightarrow[\text{slow}]{k_{\mathrm{VIII,X}}} [\mathrm{Cr(OH)_{X-1}(R)(H_2O)_{4-X}}]^{(3-X)+} + \mathrm{H_2O} \tag{43}$$

$$[\mathrm{Cr(OH)_{X-1}(R)(H_2O)_{4-X}}]^{(3-X)+} + \mathrm{OH^-} \xrightarrow{k_{\mathrm{IX,X}}} [\mathrm{Cr(OH)_X(R)(H_2O)_{4-X}}]^{(2-X)+} \tag{44}$$

$$[\mathrm{Cr(OH)_{X-1}(R)(H_2O)_{4-X}}]^{(3-X)+} + \mathrm{H_2O} \xrightarrow{k_{\mathrm{X,X}}} [\mathrm{Cr(OH)_{X-1}(R)(H_2O)_{5-X}}]^{(3-X)+} \tag{45}$$

$$[Cr(OH)_{x-1}(R)(H_2O)_{4-x}]^{(3-x)+} + RH \xrightarrow{k_{XI,x}} [Cr(OH)_{x-1}(R)(RH)(H_2O)_{4-x}]^{(3-x)+} \quad (46)$$

Assuming again that the penta-coordinated intermediate is reactive enough to be in steady state, the following expression can be obtained for the second experimental rate constant:

$$k_2 = \frac{\sum_{x=1}^{3} k_{2,x} [Cr(OH)_{x-1}(R)(H_2O)_{5-x}^{(3-x)+}]}{\sum_{x=1}^{3} [Cr(OH)_{x-1}(R)(H_2O)_{5-x}^{(3-x)+}]} \quad (47)$$

where:

$$k_{2,x} = \frac{k_{VIII,x}\ k_{XI,x}\ [RH]}{k_{IX,x}\ [OH^-] + k_{X,x} + k_{XI,x}\ [RH]} \quad (48)$$

Equations 47 and 48 are consistent with the dependence of k_2 on the initial concentration of organic ligand (fractional kinetic order, Figure 7, right). Moreover, the decreasing effect of the ionic strength (Figure 8, right) and the increasing effect of the pH (Figure 9, right) might be explained by the change in the relative proportions of the long-lived intermediates of the type $[Cr(OH)_{x-1}(R)(H_2O)_{5-x}]^{(3-x)+}$, provided that $k_{VIII,x}$ increases gradually from x = 1 to 3 (the hydroxo ligands render the Cr-H_2O bonds more labile), addition of a background electrolyte resulting in an increase of the contributions of the less reactive, lower-x species (through a shift of the acid-dissociation equilibria of the long-lived intermediates to the left side because the reaction products are like-charged ions), whereas an increase of the pH resulted in an increase of the contributions of the more reactive, higher-x species.

Given enough time (at $t = \infty$), the following equilibria might be reached:

$$[Cr(OH)_{x-1}(R)(RH)(H_2O)_{4-x}]^{(3-x)+} \underset{H_2O}{\overset{RH}{\rightleftharpoons}} [Cr(OH)_{x-1}(R)(RH)_2(H_2O)_{3-x}]^{(3-x)+} \quad (49)$$

$$[Cr(OH)_{x-1}(R)(RH)(H_2O)_{4-x}]^{(3-x)+} + H_3O^+ \rightleftharpoons [Cr(OH)_{x-1}(RH)_2(H_2O)_{5-x}]^{(4-x)+} \quad (50)$$

$$[Cr(OH)_{x-1}(R)(RH)_2(H_2O)_{3-x}]^{(3-x)+} + H_3O^+ \rightleftarrows [Cr(OH)_{x-1}(RH)_3(H_2O)_{4-x}]^{(4-x)+} \quad (51)$$

the correspondence between the complexes appearing in eqs 49 – 51 and those seen before in eqs 20 and 21 being as that shown in Table 5.

Predicted complex	Proposed complex
C_n	$[Cr(OH)_{x-1}(R)(RH)(H_2O)_{4-x}]^{(3-x)+}$
$C_n - H^+$	$[Cr(OH)_{x-1}(RH)_2(H_2O)_{5-x}]^{(4-x)+}$
C_{n+1}	$[Cr(OH)_{x-1}(R)(RH)_2(H_2O)_{3-x}]^{(3-x)+}$
$C_{n+1} - H^+$	$[Cr(OH)_{x-1}(RH)_3(H_2O)_{4-x}]^{(4-x)+}$

(a) The subscripts n and $n+1$ stand for the number of organic ligands.
(b) RH and R stand for amino acid molecules acting as mono- or bi-dentate ligands, respectively.

Table 5. Correspondence between the symbols of the final violet complexes predicted from their recorded UV-Vis spectra and the chemical formulas proposed in the mechanism.

The number of hydrogen ions released to the medium during the course of the reaction (per chromium atom belonging to the violet complex) can then be estimated as:

$$\text{Number } (H^+) = \frac{x\,([C_n] + [C_{n+1}]) + (x-1)\,([C_n - H^+] + [C_{n+1} - H^+])}{[Cr(III)]_T} \quad (52)$$

and, depending on the experimental conditions, it takes values in the range $0 < \text{Number } (H^+) < 3$ (since $x = 1\text{-}3$), in agreement with Figures 12 and 13.

Finally, we can conclude that, all in all, and considering the complexity of the chemical problem under study, the kinetic model used to obtain the reaction parameters should be considered as a good enough approximation to the real behavior of nature.

13. CONCLUSIONS

(i) The reaction rate decreased much faster than expected for a pseudo-first order process (even under a large excess of organic ligand). This unusual pattern could be explained by the participation of a long-lived intermediate, not being reactive enough for the steady-state approximation to apply, and the rate constants corresponding to the formation (k_1) and decay (k_2) of the long-lived intermediate have been determined under different experimental conditions.

(ii) Rate constant k_1 was one order of magnitude higher than k_2, and the respective activation energies were 60.2 ± 3.3 and 83.3 ± 5.9 kJ mol^{-1}, indicating that the formation of the long-lived intermediate was much faster than its decay.

(iii) The UV-Vis spectrum of the long-lived intermediate was intermediary between those of the green inorganic reactant and the violet reaction product, whereas the spectroscopy data strongly suggested the coexistence of at least four complexes between Cr(III) and L-alanine in the final reacting mixture, differing in the number of organic ligands as well as in their acid-base properties.

(iv) The rate constants for the replacement of an aqua ligand by L-alanine at 25.0 ºC followed the sequence $CrOH^{2+}$ (1.77 M^{-1} s^{-1}) < $Cr(OH)_2^+$ (128 M^{-1} s^{-1}) < $Cr(OH)_3$ (3.07 × 10^4 M^{-1} s^{-1}), revealing that the hydroxo ligands rendered the Cr(III)-H_2O chemical bonds more labile.

(v) A reaction mechanism, consistent with the available experimental information, has been proposed, including an elementary reaction sequence for each experimental rate constant, the key (slow) steps implying the breakage of a Cr(III)-H_2O chemical bond, thus leaving a vacant coordination place to allow the entrance of the organic ligand.

14. REFERENCES

1. Nkabinde, S. V.; Kinunda, G.; Jaganyi, D. Mechanistic Study of the Substituion Reactions of [Pt(II)(bis(2-pyridylmethyl)amine)H_2O]$(ClO_4)_2$ and [Pt(II)(bis(2-pyridylmethyl)sulfide)H_2O]$(ClO_4)_2$ with Azole Nucleophiles. Crystal Structure of [Pt(II)(bis(2-pyridylmethyl)sulfide)Cl]ClO_4. *Inorg. Chim. Acta* **2017**, *466,* 298-307.
2. Bakac, A.; Espenson, J. H. Chromium Complexes Derived from Molecular Oxygen. *Acc. Chem. Res.* **1993,** *26,* 519-523.
3. Perez-Benito, J. F. Effects of Chromium(VI) and Vanadium(V) on the Lifespan of Fish. *J. Trace Elem. Med. Biol.* **2006,** *20,* 161-170.
4. Hamm, R. E. Complex Ions of Chromium. IV. The Ethylenediaminetetraacetic Acid Complex with Chromium(III). *J. Am. Chem. Soc*. **1953**, *75*, 5670-5672.
5. Perez-Benito, J. F. Two Rate Constant Kinetic Model for the Chromium(III)-EDTA Complexation Reaction by Numerical Simulations. *Int. J. Chem. Kinet.* **2017,** *49,* 234-249.
6. Hedrick, C. E. Formation of the Chromium-EDTA Complex. *J. Chem. Educ.* **1965**, *42*, 479-480.
7. Barreto, J. C.; Brown, D.; Dubetz, T.; Kakareka, J.; Alberte, R. S. A Spectrophotometric Determination of the Energy of Activation (E_a) for a Complexation Reaction: The Kinetics of Formation of a Cr(III)/EDTA Complex. *Chem. Educator* **2005**, *10*, 196-199.
8. Staniek, H.; Wojaciak, R. W. The Combined Effect of Supplementary Cr(III) Propionate Complex and Iron Deficiency on the Chromium and Iron Status in Female Rats. *J. Trace Elem. Med. Biol.* **2018,** *45,* 142-149.
9. Schwarz, K.; Mertz, W. Chromium(III) and the Glucose Tolerance Factor. *Arch. Biochem. Biophys.* **1959**, *85*, 292-295.
10. Berdicevsky, I.; Mirsky, N. Effects of Insuline and Glucose-Tolerance Factor (GTF) on Growth of Saccharomyces-Cerevisiae. Mycoses **1994,** *37,* 405-410.
11. Weksler-Zangen, S.; Mizrahi, T.; Raz, I. Glucose Tolerance Factor Extracted from Yeast: Oral Insulin-Mimetic and Insulin-Potentiating: *In Vivo* and *In Vitro* Studies. *Br. J. Nutr.* **2012,** *108,* 875-882.
12. Liu, L.; Cui, W. M.; Zhang, S. W.; Kong, F. H.; Pedersen, M. A.; Wen, Y.; Lv, J. P. Effect of Glucose Tolerance Factor (GTF) from High Chromium Yeast on Glucose Metabolism in Insulin-Resistant 3T3-L1 Adipocytes. *RSC Adv*. **2015**, *5,* 3482-3490.
13. Vincent, J. B. New Evidence Against Chromium as an Essential Trace Element. *J. Nutr.* **2017,** *147,* 2212-2219.
14. Stearns, D. M. Is Chromium a Trace Essential Metal? Biofactors **2000,** *11,* 149-162.
15. Mertz, W. Chromium in Human Nutrition. A Review. *J. Nutr.* **1993**, *123*, 626-633.
16. Garrett, R. H.; Grisham, C. M. *Biochemistry*; Cengage Learning: Boston, 2017.
17. Kitadai, N.; Oonishi, H.; Umemoto, K.; Usui, T.; Fukushi, K.; Nakashima, S. Glycine Polymerization on Oxide Minerals. *Orig. Life Evol. Biosph.* **2017**, *47*, 123-143.
18. Remko, M.; Rode, B. M. Catalyzed Peptide Bond Formation in the Gas Phase. Role of Bivalent Cations and Water in Formation of 2-Aminoacetamide from Ammonia and Glycine and in Dimerization of Glycine. *Struct. Chem.* **2004**, *15*, 223-232.
19. Khan, I. A.; Kabir-ud-Din, K. Anation of Hexaaquachromium(III) by Glycine. *J. Inorg. Nucl. Chem.* **1981**, *43*, 1082-1085.
20. Khan, I. A.; Shadid, M.; Kabir-ud-Din, K. Kinetics of Anation of Hexaaquachromium(III) Ion by Serine in Aqueous Acidic Medium. *Indian J. Chem. A* **1983**, *22*, 382-385.
21. Khan, I. A.; Kabir-ud-Din, K. Kinetics of Anation of Hexaaquachromium(III) Ion by Valine in Aqueous Acidic Medium. *Indian J. Chem. A* **1984**, *23*, 98-101.
22. Khan, I. A.; Kabir-ud-Din, K. Kinetics of Anation of Hexaaquachromium(III) Ion by Aspartic Acid – Mechanism and Activation Parameters. *Transition Met. Chem.* **1986**, *11*, 391-395.

23. Khan, I. A.; Shahid, M.; Kabir-ud-Din, K. Kinetic and Mechanistic Studies on the Complexation of Aquachromium(III) with DL-Tryptophan in Aqueous Acidic Media. *J. Chem. Soc. Dalton* **1990**, *10*, 3007-3012.
24. Khan, I. A.; Shahid, M.; Kabir-ud-Din, K. Methionine Anation of Aquachromium(III). *Transition Met. Chem.* **1991**, *16*, 18-22.
25. Guindy, N. M.; Abou-Gamra, Z. M.; Abdel-Messih, M. F. Kinetic Studies on the Complexation of Aqua Chromium(III) with DL-Leucine in Aqueous Acidic Media. *J. Chim. Phys.* **1999,** *96,* 851-864.
26. Guindy, N. M.; Abou-Gamra, Z. M.; Abdel-Messih, M. F. Kinetic Studies on the Complexation of Chromium(III) with some Amino Acids in Aqueous Acidic Medium. *Monatsh. Chem.* **2000,** *131,* 857-866.
27. Niogy, B. K.; De, G. S. Kinetics and Mechanism of Anation of Hydroxopentaaquachromium(III) Ion by DL-Phenylalanine in Aqueous Solution. *J. Indian Chem.* **1984**, *61*, 389-392.
28. Ramasami, T.; Taylor, R. S.; Sykes A. G. Evidence for a Dissociative Mechanism in the Reaction of Glycine with $Cr(NH_3)_5H_20^{3+}$. Ionic Strength Contributions (as a 1:1 Electrolyte) and Ion-Pairing (K_{IP}) Ability of the Glycine Zwitterion. *Inorg. Chem.* **1976**, *15,* 2318-2320.
29. Khan, I. A.; Kabir-ud-Din, K. Studies on the Composition and Kinetics of Chromium(III)-Alanine System. *Int. J. Chem. Kinet.* **1985**, *17*, 1263-1272.
30. Niogy, B. K.; De, G. S. Kinetics and Mechanism of Anation of Hydroxopentaaquachromium(III) Ion by DL-Alanine in Aqueous Solution. *Proc. Indian Acad. Sci. Chem. Sci.* **1983**, *92*, 153-161.
31. Volk, L.; Richardson, W.; Lau, K. H.; Hall, M.; Lin, S. H. Steady State and Equilibrium Approximations in Reaction Kinetics. *J. Chem. Educ.* **1977**, *54*, 95-97.
32. Wilkinson, F. *Chemical Kinetics and Reaction Mechanisms*; Van Nostrand Reinhold: New York, 1980.
33. Perez-Benito, J. F. Some Considerations on the Fundamentals of Chemical Kinetics: Steady State, Quasi-Equilibrium, and Transition State Theory. *J. Chem. Educ.* **2017,** *94,* 1238-1246.
34. Freeman, F.; Kappos, J. C. Permanganate Ion Oxidations. 15. Addittional Evidence for Formation of Soluble (Colloidal) Manganese Dioxide during the Permanganate Ion Oxidation of Carbon-Carbon Double Bonds in Phosphate-Buffered Solutions. *J. Am. Chem. Soc.* **1985,** *107,* 6628-6633.
35. Perez-Benito, J. F.; Arias, C. Occurrence of Colloidal Manganese Dioxide in Permanganate Reactions. *J. Colloid Interface Sci.* **1991,** *152,* 70-84.
36. Perez-Benito, J. F. Autocatalytic Reaction Pathway on Manganese Dioxide Colloidal Particles in the Permanganate Oxidation of Glycine. *J. Phys. Chem. C* **2009**, *113,* 15982-15991.
37. Espenson, J. H. *Chemical Kinetics and Reaction Mechanisms*; McGraw-Hill: New York, 1995.
38. Stünzi, H.; Marty, W. Early Stages of the Hydrolysis of Chromium(III) in Aqueous Solution. 1. Characterization of a Tetrameric Species. *Inorg. Chem.* **1983,** *22,* 2145-2150.
39. Galstyan, G.; Knapp, E. W. Computing pK_a Values of Hexa-Aqua Transition Metal Complexes. *J. Comput. Chem.* **2015,** *36,* 69-78.
40. Robinson, P. J. Dimensions and Standard States in the Activated Complex Theory of Reaction Rates. *J. Chem. Educ.* **1978**, *55*, 509-510.
41. Coetzee, J. F.; Ritchie, C. D. *Solute-Solvent Interactions*; Dekker: New York, 1969.
42. Dawson, R. M. C.; Elliott, D. C.; Elliott, W. H.; Jones, K. M. *Data for Biochemical Research*; Clarendon Press: Oxford, 1989.
43. Dhanpat, R.; Bruce, M. S.; Dean A. M. Chromium(III) Hydrolysis Constant and Solubility of Chromium(III) Hydroxide. *Inorg. Chem.* **1987,** *26,* 345-345.
44. Lopez-Gonzalez, H.; Peralta-Videa, J. R.; Romero-Guzman, E. T.; Rojas-Hernandez, A.; Gardea-Torresdey, J. L. Determination of the Hydrolysis Constants and Solubility Product of Chromium(III) from Reduction of Dichromate Solutions by ICP-OES and UV-Visible Spectroscopy. *J. Solution Chem.* **2010,** *39,* 522-532.

APPENDICES

APPENDIX 1: *Absorbance (λ_1) - absorbance (λ_2) relationships*

In order to develop the mathematical basis of the absorbance-absorbance relationships, let us start by considering the case of two consecutive reactions, involving a reactant (R), an intermediate (I) and a product (P). The corresponding mass balance requires the use of two conversion variables (extents of reactions per unit volume, x and y) at a certain instant during the course of the process:

$$\mathrm{R} \xrightarrow{x} \mathrm{I} \xrightarrow{y} \mathrm{P} \qquad (1\text{-A})$$

Assuming now the fulfillment of the Lambert-Beer law by the three chemical species, the absorbances at two different wavelengths measured at the same instant during the course of the reaction can be calculated as the sum of the independent contributions of each substance:

$$A(\lambda_1) = \varepsilon_{\mathrm{R},1}\, l\, [\mathrm{R}] + \varepsilon_{\mathrm{I},1}\, l\, [\mathrm{I}] + \varepsilon_{\mathrm{P},1}\, l\, [\mathrm{P}] \qquad (2\text{-A})$$

$$A(\lambda_2) = \varepsilon_{\mathrm{R},2}\, l\, [\mathrm{R}] + \varepsilon_{\mathrm{I},2}\, l\, [\mathrm{I}] + \varepsilon_{\mathrm{P},2}\, l\, [\mathrm{P}] \qquad (3\text{-A})$$

where the subscripts of the molar absorption coefficients (ε) indicate the respective species and wavelength, l being the optical path length (1 cm). The concentrations at a certain instant are given by the equations:

$$[\mathrm{R}] = [\mathrm{R}]_\mathrm{o} - x \qquad [\mathrm{I}] = x - y \qquad [\mathrm{P}] = y \qquad (4\text{-A})$$

where $[\mathrm{R}]_\mathrm{o}$ is the reactant initial concentration. Finally, from eqs 2-A to 4-A, it follows that:

$$A(\lambda_1) = A(\lambda_1)_\mathrm{o} + \frac{\varepsilon_{\mathrm{P},1} - \varepsilon_{\mathrm{R},1}}{\varepsilon_{\mathrm{P},2} - \varepsilon_{\mathrm{R},2}} \left[A(\lambda_2) - A(\lambda_2)_\mathrm{o}\right] + f(\mathrm{I}) \qquad (5\text{-A})$$

$$f(\mathrm{I}) = \left[\frac{\varepsilon_{\mathrm{I},1} (\varepsilon_{\mathrm{P},2} - \varepsilon_{\mathrm{R},2}) + \varepsilon_{\mathrm{P},1} (\varepsilon_{\mathrm{R},2} - \varepsilon_{\mathrm{I},2}) + \varepsilon_{\mathrm{R},1} (\varepsilon_{\mathrm{I},2} - \varepsilon_{\mathrm{P},2})}{\varepsilon_{\mathrm{P},2} - \varepsilon_{\mathrm{R},2}} \right] l\,[\mathrm{I}] \quad \text{(6-A)}$$

$A(\lambda_1)_o = \varepsilon_{R,1}\, l\, [R]_o$ and $A(\lambda_2)_o = \varepsilon_{R,2}\, l\, [R]_o$ being the initial absorbances of the reactant mixture at the two considered wavelengths (since $[I]_o = [P]_o = 0$).

Given that a plot of the intermediate concentration as a function of time shows an increasing period at the beginning, a maximum and a final decreasing period, it is indeed clear that eqs 5-A and 6-A lead to a nonlinear $A(\lambda_1)$ vs. $A(\lambda_2)$ graphical representation. Nonetheless, a linear behavior can be obtained simply by assuming that the intermediate is reactive enough to be in negligible concentration (that is, in steady state). Effectively, by replacing $[I] = 0$ in eqs 5-A and 6-A, it can be deduced that:

$$A(\lambda_1) = A(\lambda_1)_o + \frac{\varepsilon_{\mathrm{P},1} - \varepsilon_{\mathrm{R},1}}{\varepsilon_{\mathrm{P},2} - \varepsilon_{\mathrm{R},2}} \left[A(\lambda_2) - A(\lambda_2)_o \right] \quad \text{(7-A)}$$

leading this time to a linear $A(\lambda_1)$ vs. $A(\lambda_2)$ plot.

Now, we have enough mathematical background to be able to interpret the absorbance-absorbance relationships observed in the particular case of the Cr(III)-alanine reaction, for which the graphical representations of the absorbances at 400 and 585 nm as a function of that at 530 nm led to upward-concave (Figure 2, right) and downward-concave (Figure 2, left) curvatures, respectively.

Therefore, the finding of nonlinear absorbance-absorbance plots (instead of straight lines) allows us concluding that eqs 5-A and 6-A (instead of eq 7-A) are the ones describing the real behavior of our reaction. Hence, at least one long-lived intermediate must necessarily be involved in the mechanism.

APPENDIX 2: *Tabulated experimental kinetic data*

$[Cr(NO_3)_3]_o$ [10^{-2} M]	pH	k_1 [10^{-4} s^{-1}]	k_2 [10^{-5} s^{-1}]	E [10^{-4}]
0.59	4.12 ± 0.01	3.73 ± 0.04	5.08 ± 0.24	5.28± 0.14
0.88	3.96 ± 0.01	2.64 ± 0.03	4.03 ± 0.17	4.27 ± 0.24
1.18	3.86 ± 0.02	1.83 ± 0.04	3.16 ± 0.39	6.61 ± 1.25
1.47	3.78 ± 0.03	1.40 ± 0.01	2.58 ± 0.22	7.32 ± 0.70
1.76	3.72 ± 0.01	0.89 ± 0.06	1.38 ± 0.30	7.93 ± 0.23

(a) The pH values were measured at the end of the reaction.
(b) *E* is the average error of the theoretical absorbances with respect to the experimental ones.

Table 1-A. Values of the experimental rate constants at different metal ion initial concentrations. [L-alanine]$_o$ = 0.354 M, [KOH]$_o$ = 5.03 × 10^{-3} M, 25.0 ºC.

$[KNO_3]$ [M]	Ionic strength [M]	pH	k_1 [10^{-4} s^{-1}]	k_2 [10^{-5} s^{-1}]	E [10^{-4}]
0.000	0.040	4.12 ± 0.01	3.73 ± 0.04	5.08 ± 0.24	5.28± 0.14
0.029	0.069	4.13 ± 0.01	4.24 ± 0.01	4.88 ± 0.33	7.49 ± 0.60
0.059	0.099	4.16 ± 0.01	4.53 ± 0.29	4.63 ± 0.32	10.03 ± 0.73
0.088	0.129	4.18 ± 0.01	4.89 ± 0.19	4.81 ± 0.32	9.57 ± 0.14
0.118	0.158	4.20 ± 0.01	4.69 ± 0.19	4.43 ± 0.34	10.01 ± 0.53

(a) The pH values were measured at the end of the reaction.
(b) *E* is the average error of the theoretical absorbances with respect to the experimental ones.

Table 2-A. Values of the experimental rate constants at different concentrations of potassium nitrate. $[Cr(NO_3)_3]_o$ = 5.88 × 10^{-3} M, [L-alanine]$_o$ = 0.354 M, [KOH]$_o$ = 5.03 × 10^{-3} M, 25.0 ºC.

$[L\text{-alanine}]_o$ [M]	pH	k_1 [10^{-4} s^{-1}]	k_2 [10^{-5} s^{-1}]	E [10^{-4}]
0.015	3.87 ± 0.03	1.62 ± 0.09	1.69 ± 0.01	3.85 ± 0.01
0.030	3.84 ± 0.03	1.96 ± 0.14	2.42 ± 0.05	4.10 ± 0.13
0.044	3.86 ± 0.01	2.33 ± 0.42	2.94 ± 0.43	4.38 ± 0.29
0.059	3.79 ± 0.05	3.19 ± 0.16	3.19 ± 0.09	5.59 ± 0.44
0.074	3.87 ± 0.02	3.35 ± 0.05	3.65 ± 0.36	6.58 ± 0.46
0.088	3.89 ± 0.01	2.98 ± 0.31	3.40 ± 0.01	7.15 ± 0.27
0.103	3.90 ± 0.01	3.38 ± 0.02	3.72 ± 0.05	9.56 ± 0.77
0.118	3.96 ± 0.02	2.98 ± 0.03	3.66 ± 0.16	7.51 ± 2.34
0.133	3.97 ± 0.01	3.64 ± 0.19	3.87 ± 0.01	8.01 ± 0.71
0.184	4.02 ± 0.02	3.86 ± 0.76	4.89 ± 0.60	9.25 ± 1.00
0.235	4.09 ± 0.02	5.22 ± 0.01	5.93 ± 0.20	8.20 ± 2.01
0.294	4.16 ± 0.01	5.08 ± 0.07	5.98 ± 0.24	14.82 ± 0.17
0.354	4.24 ± 0.02	6.15 ± 0.21	6.30 ± 0.06	14.12 ± 0.59

(a) The pH values were measured at the end of the reaction.
(b) *E* is the average error of the theoretical absorbances with respect to the experimental ones.

Table 3-A. Values of the experimental rate constants at different L-alanine initial concentrations.

$[Cr(NO_3)_3]_o = 5.88 \times 10^{-3}$ M, $[KOH]_o = 8.28 \times 10^{-3}$ M, 25.0 ºC.

$[KOH]_o$ [10^{-3} M]	pH	k_1 [10^{-5} s^{-1}]	k_2 [10^{-6} s^{-1}]	E [10^{-4}]
1.64	3.56 ± 0.01	2.20 ± 0.25	4.03 ± 0.54	3.64 ± 0.16
3.28	3.61 ± 0.01	3.01 ± 0.02	6.73 ± 1.00	3.44 ± 0.03
4.93	3.70 ± 0.01	6.26 ± 0.13	4.23 ± 0.65	4.14 ± 0.44
6.57	3.71 ± 0.01	12.62 ± 0.11	8.45 ± 1.49	4.27 ± 0.39
8.21	3.84 ± 0.01	24.39 ± 1.01	25.92 ± 0.91	7.09 ± 0.92

(a) The pH values were measured at the end of the reaction.
(b) *E* is the average error of the theoretical absorbances with respect to the experimental ones.

Table 4-A. Values of the experimental rate constants at different potassium hydroxide initial concentrations. $[Cr(NO_3)_3]_o = 5.88 \times 10^{-3}$ M, $[\text{L-alanine}]_o = 5.89 \times 10^{-2}$ M, 25.0 ºC.

Temperature [ºC]	k_1 [10^{-4} s^{-1}]	k_2 [10^{-5} s^{-1}]	E [10^{-4}]
20.0	2.59 ± 0.01	2.63 ± 0.01	5.54 ± 0.76
22.5	3.02 ± 0.03	3.30 ± 0.06	6.79 ± 0.42
25.0	3.73 ± 0.04	5.08 ± 0.24	5.28 ± 0.14
27.5	4.72 ± 0.01	6.03 ± 0.29	6.95 ± 1.34
30.0	5.77 ± 0.49	8.03 ± 0.97	6.30 ± 2.71

(a) *E* is the average error of the theoretical absorbances with respect to the experimental ones.

Table 5-A. Values of the experimental rate constants at different temperatures. $[Cr(NO_3)_3]_o = 5.88 \times 10^{-3}$ M, $[\text{L-alanine}]_o = 0.354$ M, $[KOH]_o = 5.03 \times 10^{-3}$ M, pH_∞ 4.06 ± 0.03.

APPENDIX 3: *Four complexes in equilibrium: mathematical basis*

Let us consider the four Cr(III)-alanine complexes involved in eqs 20 and 21, the corresponding equilibrium constants being:

$$K_1 = \frac{[C_{n+1} - H^+]}{[C_n - H^+]\,[Ala]} \quad (8\text{-A})$$

$$K_2 = \frac{[C_{n+1}]}{[C_n]\,[Ala]} \quad (9\text{-A})$$

Now, a mass balance for Cr(III) allows us to write:

$$[Cr(III)]_T = [C_n - H^+] + [C_{n+1} - H^+] + [C_n] + [C_{n+1}] \quad (10\text{-A})$$

where $[Cr(III)]_T$ stands for the total concentration of metal ion. From eqs 8-A to 10-A, it follows that:

$$[Cr(III)]_T = (1 + K_1\,[Ala])\,[C_n - H^+] + (1 + K_2\,[Ala])\,[C_n] \quad (11\text{-A})$$

For their part, the concentrations of the C_n–H^+ and C_n species are related by the following acid-dissociation equilibrium:

$$C_n - H^+ \xrightleftharpoons{K_3} C_n + H^+ \quad (12\text{-A})$$

the corresponding acidity constant being:

$$K_3 = \frac{[C_n]\,[H^+]}{[C_n - H^+]} \quad (13\text{-A})$$

From eqs 8-A, 9-A, 11-A and 13-A, it follows that:

$$[C_n - H^+] = \frac{[Cr(III)]_T\,[H^+]}{(1 + K_1\,[Ala])\,[H^+] + K_3\,(1 + K_2\,[Ala])} \quad (14\text{-A})$$

$$[C_{n+1} - H^+] = \frac{K_1 [Cr(III)]_T [H^+] [Ala]}{(1 + K_1 [Ala]) [H^+] + K_3 (1 + K_2 [Ala])} \quad (15\text{-A})$$

$$[C_n] = \frac{K_3 [Cr(III)]_T}{(1 + K_1 [Ala]) [H^+] + K_3 (1 + K_2 [Ala])} \quad (16\text{-A})$$

$$[C_{n+1}] = \frac{K_2 K_3 [Cr(III)]_T [Ala]}{(1 + K_1 [Ala]) [H^+] + K_3 (1 + K_2 [Ala])} \quad (17\text{-A})$$

and dividing member by member eqs 14-A and 15-A on one hand:

$$\frac{[C_{n+1} - H^+]}{[C_n - H^+]} = K_1 [Ala] \quad (18\text{-A})$$

and eqs 16-A and 17-A on the other:

$$\frac{[C_{n+1}]}{[C_n]} = K_2 [Ala] \quad (19\text{-A})$$

It should be observed that [Ala] represents the concentration of free L-alanine. A mass balance for the organic reactant will allow us to evaluate how much of it is present in the free form and how much in the ligand form, the total concentration being:

$$[Ala]_T = [Ala] + n[C_n]_T + (n+1)[C_{n+1}]_T \quad (20\text{-A})$$

where:

$$[C_n]_T = [C_n] + [C_n - H^+] \quad (21\text{-A})$$

$$[C_{n+1}]_T = [C_{n+1}] + [C_{n+1} - H^+] \quad (22\text{-A})$$

From eqs 18-A to 20-A, it is easy to infer eqs 22 and 23, in perfect agreement with the experimental information inferred from the UV-Vis spectra recorded for the final reacting mixtures.

APPENDIX 4: *Changing the optical isomer: racemic mixture*

When the source of organic ligands was changed from L-alanine to a DL-alanine racemic mixture, both the kinetic data (k_1 and k_2, Figure 1-A, left) and the final UV-Vis spectrum (Figure 1-A, right) remained unaltered within the experimental error margin, denoting that the reaction was rather insensitive to the nature of the amino acid optical isomer.

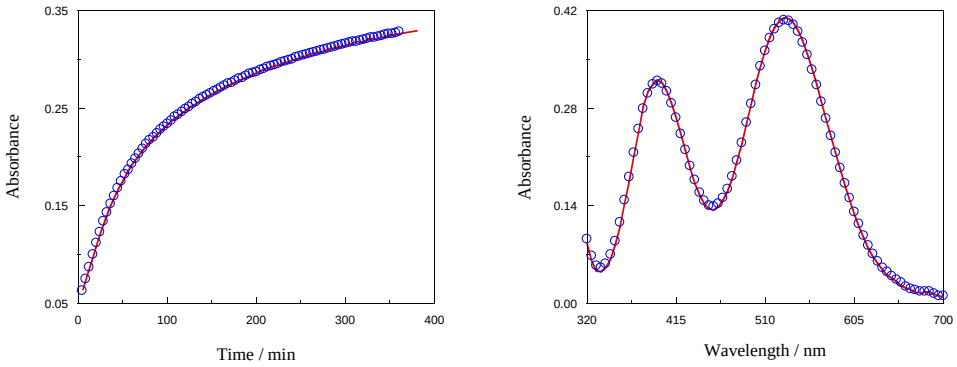

Figure 1-A. Absorbance at 530 nm as a function of time (left) and UV-Vis spectrum (right) with either L-alanine (blue points) or DL-alanine racemic mixture (red line) as source of organic ligands. $[Cr(NO_3)_3]_o$ = 5.88×10^{-3} M, $[ligand]_o$ = 0.354 M, $[KOH]_o$ = 5.00×10^{-3} M, pH_∞ 4.10 ± 0.02, 25.0 ºC.

This result was not indeed unexpected as far as the first experimental rate constant (k_1) is concerned, since the symmetry of the inorganic reactant precludes its possibility to differentiate between the L and D isomers of the amino acid (the contrary would violate the physical principle of symmetry conservation). However, given the asymmetry of the long-lived intermediate (with chromium coordinated to either L- or D-alanine), the absence of any appreciable effect on neither rate constant k_2 or the final UV-Vis spectrum suggests that two or more organic ligands can coexist in the same complex regardless of the optical form of each ligand, the optical isomerism not affecting either the reactivity of the long-lived intermediate or the stability of the final product, the bi-coordinated complexes of the types LL or DD being formed with the same probability as those of the type LD.